Limited effect of basalt amendment and mycorrhizal inoculation on soil chemical properties and maize growth on a nutrient-rich soil

Lucilla Boito[1]*, Jet Rijnders[1]*, Laura Steinwidder[1], Patrick Frings[2], Arthur Vienne[1], Mirthe Maes[3], Erik Verbruggen[3], Sara Vicca[1]

[1]Biobased Sustainability Engineering (SUSTAIN), Department of Bioscience Engineering, University of Antwerp, Antwerp, 2020, Belgium
[2]Earth Surface Geochemistry, German Research Centre for Geosciences (GFZ), Potsdam, 14473, Germany
[3]Plants and Ecosystems (PLECO), Department of Biology, University of Antwerp, Wilrijk, 2610, Belgium

Correspondence to: Lucilla Boito, Sara Vicca (lucilla.boito@uantwerpen.be; sara.vicca@uantwerpen.be)

*Both authors contributed equally to this work

Abstract. Enhanced weathering (EW) of silicate minerals has emerged as a promising carbon dioxide removal (CDR) strategy, with potential benefits for soil fertility and crop performance. However, the soil processes that determine these co-benefits remain poorly explained. In particular, interactions between basalt amendments and soil biota such as arbuscular mycorrhizal fungi (AMF) may influence nutrient mobilization and plant uptake, but these effects have rarely been quantified. In a 113-day mesocosm experiment with *Zea mays* using a Belgian, sandy loam Plaggic anthrosoil (pH = 5.6), we investigated the effect of basalt (applied at 50 ton ha^{-1}) and AMF inoculation on soil properties, nutrient and heavy metal availability, and crop yield and quality. We also assessed potential AMF-driven bio-weathering via cation mass balance and pore water dissolved inorganic carbon (DIC), pH, and alkalinity measurements. In our experiment, basalt application, but not AMF, improved soil pH (+0.71 ± 0.14), cation exchange capacity (+0.43 ± 0.18 meq 100 g^{-1}), base saturation (+13.6 ± 3.5 %), and generally increased exchangeable Ca and Mg in the 0-40 cm soil profile (+80.2 ± 24.6 and + 23.9 ± 4.4 mg kg $soil^{-1}$ respectively), whereas most other nutrients in the pore water remained unaffected (all values are mean ± SE). Crop yield and quality were largely unaltered by basalt or AMF, except for an increase in plant Mg with basalt application. Moreover, heavy metal availability and plant uptake were also generally unaffected, with the notable exception of soil pore water and corn Ni, which increased with basalt (+0.02 ± 0.005 mg l^{-1}; +0.0002 ± 0.0001 mg g dry $biomass^{-1}$; mean ± SE). These results suggest that risks associated with heavy metal contamination are not generic, but may depend on local soil conditions. In our experiment, elevated background Ni concentrations likely contributed to pore water Ni concentrations exceeding the environmental quality standards of the EU and Australia even in the control treatments. Finally, we found no clear evidence that AMF enhanced basalt weathering rates. Overall, AMF had limited influence on soil chemical fertility and crop performance. On the other hand, basalt application improved key soil chemical indicators and increased the exchangeable fractions of Ca and Mg, demonstrating its role as a soil improver. Unlike several studies conducted in more acidic soils however, these chemical enhancements did not increase maize growth here, suggesting limited short-term agronomic benefits of basalt under the fertile soil studied here.

1 Introduction

Amidst the urgent need for sustainable agricultural practices in the face of climate change (Branca et al., 2013), enhanced weathering (EW) of silicate minerals emerges as a promising solution, offering a novel approach to mitigate carbon dioxide (CO_2) levels while simultaneously improving soil health and crop yields (Swoboda et al., 2022). Silicate minerals react with water and CO_2 to form (bi)carbonate, resulting in long-term carbon (C) sequestration (Dietzen et al., 2018; Moosdorf et al., 2014). This is a naturally occurring process that regulates the global C cycle over geological timescales, but it is too slow to cope with the current rising atmospheric CO_2 concentrations (Goudie and Viles, 2012). EW aims to accelerate this natural process by grinding the silicate rocks into a fine powder in order to increase their surface area and hence their weathering rate (Renforth et al., 2011). When applied to soils, this process is facilitated by moisture, elevated CO_2 concentrations, and microbial activity.

Beyond its carbon dioxide removal (CDR) potential, EW can affect soil chemical fertility and crop performance. Silicate weathering releases nutrients, can counterbalance soil acidification, and improve soil water retention and cation exchange capacity (Swoboda et al., 2022; Van Straaten, 2006). Moreover, weathering of silicate minerals releases divalent metal cations and promotes the formation of secondary clay-sized minerals, both of which can facilitate the stabilization of soil organic matter through organo-mineral interactions (Kleber et al., 2015; Slessarev et al., 2021; Wu et al., 2023), potentially improving soil fertility (Oldfield et al., 2019; Woomer et al., 1994). In line with this, EW has been shown to stimulate plant growth and crop yield, particularly in acidic or nutrient-depleted soils (Goll et al., 2021; Shamshuddin et al., 2011; Vaghetti Luchese et al., 2021), whereas responses in fertile agricultural soils have been less positive (Swoboda et al., 2022).

On the other hand, EW may also introduce undesirable side effects. These include the accumulation of heavy metals and reduced water infiltration, potentially resulting from the occlusion of (macro)pores by rock amendments which limit preferential flow pathways (Akortey et al., 2026; Dupla et al., 2023). Additionally, increases in soil pH may stimulate microbial activity, potentially accelerating organic matter decomposition and leading to net losses of soil organic carbon (SOC; Wang and Kuzyakov, 2024). Such SOC losses could not only reduce soil fertility, but also partly offset the carbon sequestration benefits of EW, as gains in inorganic carbon storage may occur at the expense of organic carbon stocks (Buss et al., 2024; Lei et al., 2025; Steinwidder et al., 2025). Consequently, these processes could diminish both the agronomic and CDR benefits anticipated from EW. However, the mechanisms governing these co-benefits and risks remain insufficiently explained, particularly the biotic interactions that may modulate EW effects in soils.

Basalt is often considered for agricultural soil amendment due to its widespread availability and mineral composition. As an igneous rock rich in magnesium and iron silicates, it can also contain essential macronutrients such as calcium and potassium, along with important micronutrients and beneficial elements such as silicon (Conceição et al., 2022). Compared

to other (ultra)mafic silicate rocks like dunite, basalt contains lower concentrations of toxic heavy metals such as nickel and chromium, making it a safer option for agricultural use (Amann et al., 2020; Swoboda et al., 2022). Nevertheless, such risks are not negligible, given the substantial heterogeneity in basalt's elemental composition, which may lead to heavy metal concentrations spanning from safe to potentially concerning levels (Dupla et al., 2023). On the other hand, the bioavailability of heavy metals is also strongly influenced by pH, with higher pH generally reducing the solubility and uptake of metals like nickel and zinc (Basta et al., 1993). Basalt application may thus improve soil chemical fertility while minimizing contamination risks, although local soil conditions, as well as feedstock selection and application rates, can impact these outcomes.

Among soil biota, mycorrhizal symbionts, broadly classified in ectomycorrhiza and arbuscular mycorrhizal fungi (AMF), play a central role in plant nutrition and soil processes. Ectomycorrhizal associations typically occur between the fine feeder roots of woody perennial species and a relatively specific group of soil fungi (Smith and Read, 2010), and are therefore largely irrelevant for most annual cropping systems. In contrast, approximately 80 % of terrestrial plant species, including many important crops such as maize, wheat, and soybean, engage in a symbiotic relationship with AMF via their root systems (Verbruggen and Toby Kiers, 2010; Wilkes, 2021). AMF extend beyond the root surface through extensive extraradical hyphal networks, with hyphal lengths commonly on the order of 0.5 to 5 m g $soil^{-1}$ (Johnson et al., 2003; Sochorová et al., 2016), although substantially higher values (around 70 m of hyphae per g of $soil^{-1}$) have occasionally been reported (Miller et al., 1995). By exploring soil volumes inaccessible to roots alone, these networks enhance the uptake of nutrients, particularly relatively immobile elements such as phosphorus (Ferrol et al., 2019; Smith et al., 2011). The acquired nutrients are delivered to the host plant via arbuscules, AMF structures that are formed inside the root cells of the host plant (Parniske, 2008). In exchange, AMF receive carbohydrates that can be used for their growth (Kalamulla et al., 2022; Parniske, 2008; Verbruggen et al., 2021). Besides nutrient exchange, AMF can also influence soil structure and aggregation by exudation, hyphal turnover and enmeshment of soil particles (Rillig et al., 2015).

AMF can also affect the natural weathering of mineral rocks through several physical and chemical processes. Hyphae exert physical pressure on minerals, widening existing cracks and increasing their reactive surface area (Koele et al., 2014; Smits and Wallander, 2017). AMF also act as a sink for weathering products, and thus create chemical disequilibria across the rock surface which can enhance its weathering (Quirk et al., 2015; Verbruggen et al., 2021). In addition, during ammonium uptake AMF release protons that acidify the soil surroundings, thus aiding the natural weathering process (Neumann and George, 2010; Taylor et al., 2009). AMF respiration also increases CO_2 concentration in the soil (Moyano et al., 2007; Taylor et al., 2009), thereby creating a more favourable environment for rock weathering (Winnick and Maher, 2018). Finally, AMF may influence the bioavailability and plant uptake of heavy metals through acidification and glomalin-mediated chelation (Gonzalez-Chavez et al., 2004; Riaz et al., 2021).

Despite the important role of AMF in promoting nutrient uptake as well as mineral weathering, experimental evidence on the interaction between AMF and EW is limited, as highlighted by Verbruggen et al. (2021). In this study, a mesocosm experiment was established with the aim of exploring the interaction between AMF and EW in agriculture. We hypothesized that i) AMF presence increases basalt weathering rates, and thus higher dissolved inorganic carbon (DIC) and alkalinity concentrations in the pore water and base cations in the soil-water complex are expected; ii) basalt application improves soil chemical fertility and therefore plant growth and nutrient uptake, and that this effect is modulated by AMF; iii) basalt application does not increase heavy metal availability due to pH buffering, while AMF may counteract this effect through rhizosphere acidification and further affect heavy metal dynamics by altering nutrient and metal transport between soil and plant; iv) AMF growth responds to basalt application as a result of changes in soil nutrients and chemical fertility. Importantly, this study was conducted using a fertilized sandy loam soil with moderate acidity and relatively high nutrient availability, contrasting with the more acidic or nutrient-poor soils in which positive crop responses to silicate amendments are frequently reported.

2 Materials and Methods

2.1 Experimental set-up

Twenty mesocosms (0.6 m height, 0.25 m radius) were constructed at the experimental site in the Drie Eiken Campus of the University of Antwerp, Belgium (51° 9.6967' N, 4° 24.5132' E), and placed outdoors to receive natural rainfall. To allow leachate collection, a 2 cm hole at the bottom of each mesocosm was connected via polyurethane tubing to a glass collector (2.3 l). To prevent soil from leaching into the glass collector, a soil exclusion mat (black woven polypropylene; weight = 100 g m^{-2}; BRICO Belgium) covered the bottom of each mesocosm.

The experimental treatments were randomized within the facility in order to minimize differences in sun exposure, and mesocosms were wrapped in reflective foil to avoid excessive heating. In order to compare treatments with and without AMF, all soil was pasteurized by heating for 4 h at 80 °C (Ven et al., 2019; Verlinden et al., 2018). This procedure was intended to substantially reduce the abundance of fungal propagules, particularly AMF spores, while avoiding complete sterilization of the soil. AMF colonization and hyphal length results at the end of the experiment confirmed that pasteurization succeeded, as treatments that were not inoculated (see further) showed clearly lower hyphal length and colonization (Fig. 1).

The bottom 40 cm of all mesocosms was filled with a pasteurized Plaggic anthrosol soil with sandy loam texture (69.5 % sand, 28.1 % silt, 1.8 % clay; Table S1) originating from a pasture in Zandhoven, Belgium. The initial soil was slightly acidic (mean pH ± SE = 5.6 ± 0.3; soil : water = 1:2.5, see further for detailed method), with an organic carbon content of 0.8 ± 0.05% (mean ± SE; determined by loss-on-ignition at 550 °C for 4 h) and a potential cation exchange capacity (CEC) of 3.9 ± 0.6 meq 100 g $soil^{-1}$ (mean ± SE; see further for method). On 23 May 2022, the top 20 cm was filled with non-amended, pasteurized soil for the control treatments (n = 10 mesocosms). To mimic amendment incorporation through ploughing, the top 20 cm of the basalt treatments (n = 10 mesocosms) received pasteurized soil with a mixture of 0.98 kg (equivalent to 50 ton ha^{-1}) of freshly mined Eifel Basalt (Table 1; Rheinischen Provinzial-Basalt- un Lavawerke (RPBL); 50° 41.4833' N, 7° 19.1198' E), with particle size between 0.02 and 0.2 mm (Fig. S1) and specific surface area (SSA) corresponding to 6.283 ± 0.001 $m^2 g^{-1}$ (mean ± SE) measured on three technical replicates with a Quantachrome Autosorb iQ

Table 1: Left: basalt mineral phases obtained via XRD analysis on samples milled in ethanol for 10 minutes (Bruker D8 Advance, Cu Kα radiation at 30 mA and 40 kV, 2θ from 5° to 70°). An internal standard (10 wt% Al_2O_3) was added during sample preparation to determine amorphous phase content. Right: elemental concentrations obtained via XRF analysis, provided by RPBL.

Mineral	**Mineral Formula**	**Basalt**		**Basalt**
		%		%
SILICATES			Si	20.8
K-feldspar	$KAlSi_3O_8$	6.7	Mg	7.8
Plagioclase	$(Na,Ca)(Si,Al)_4O_8$	7.5	Fe	4.1
Clinopyroxene	$(Ca,Na)(Mg,Fe,Al,Ti)(Si,Al)_2O_6$	28.8	Al	3.0
Olivine	$(Mg,Fe)_2SiO_4$	13.6	Ca	7.7
Nepheline	$(Na,K)AlSiO_4$	4.2	Na	1.0
Sodalite	$Na_8Al_6Si_6O_{24}Cl_2$	1.4	Ti	1.4
Analcime	$NaAlSi_2O_6•(H_2O)$	1.9	P	0.1
2:1 layer silicates	$(K,H_3O)(Al,Mg,Fe)_2(Si,Al)_4O_{10}[(OH)_2,H_2O]$	9.1	K	0.3
		73.3	Mn	0.2
CARBONATES				
Calcite	$CaCO_3$	0.1		
OTHER/AMORPHOUS				
Amorphous		26.6		

using the Braunauer-Emmet-Teller method. The measurement used nitrogen (N_2) as adsorbate with multi-point (5 points) and isotherm (77 K) settings. The samples were degassed at 300 °C with 200 minutes of soak time. High measurement quality was ensured by frequent reference (Bundesanstalt für Materialforschung und -prüfung) measurements. Basalt
140 mineralogy was obtained through XRD analysis on samples milled in ethanol for 10 minutes (Bruker D8 Advance, Cu Kα radiation at 30 mA and 40 kV, 2θ from 5° to 70°). An internal standard (10 wt% Al_2O_3) was added during sample preparation to determine amorphous phase content. Basalt elemental composition (XRF) was provided by RPBL.

Table 2: Treatments established in the experiment, including number of replicates and abbreviations.

Treatment	Meaning	# replicates
C-AMF	Control treatment without AMF	5
C+AMF	Control treatment with AMF	5
B-AMF	50 ton ha^{-1} of basalt without AMF	5
B+AMF	50 ton ha^{-1} of basalt with AMF	5

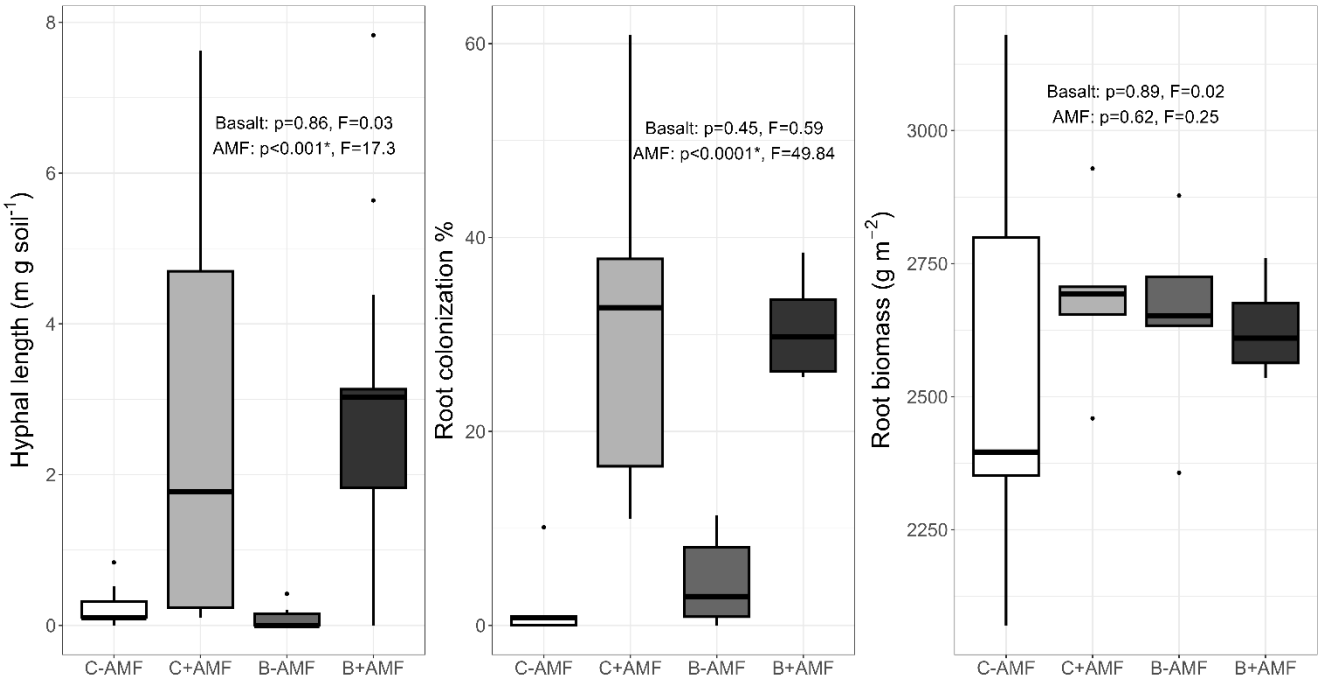


Figure 1: AMF hyphal length (a), root colonization by AMF (b) and root biomass (c) of the four treatments (C-AMF = control without AMF, C+AMF = control with AMF, B-AMF = basalt without AMF, B+AMF = basalt with AMF) at the end of the experiment. Boxes represent the interquartile range (25th-75th percentile), horizontal lines indicate the median, and whiskers extend to the most extreme data points within 1.5x of the interquartile range. Points outside this range are plotted as outliers. p- and F-values from an ANOVA analysis with hyphal length, root colonization or biomass as response variables and basalt, AMF and their interaction as covariables are shown. Interactions were not significant and were excluded from the model. Statistical significance is indicated by an asterisk (*). Compliance with model assumptions of normality and homoscedasticity was ensured by square-root transformation.

On 15 June 2022, two seeds of dwarf corn plants (*Zea mays* L., 1753; *golden midget* variety) were sown in each mesocosm to mimic a field density of about 13 plants m^{-2}. For half of the treatments (five control and five basalt mesocosms), seeds were inoculated with AMF (*Rhizophagus irregularis*; Symplanta) prior to sowing. Dry inoculum (40 g) was suspended in 200 ml of deionized water in a glass beaker and thoroughly homogenized. Seeds were subsequently added to the suspension and mixed thoroughly to ensure a uniform coating of the inoculum on the seed surface. The remaining 10 mesocosms (five control and five basalt treatments) received a sterilized inoculum (Table 2), obtained by suspending 40 g of dry inoculum in 200 ml of deionized water in a glass bottle and autoclaving the inoculum at 121 °C for 25 minutes. In addition, a microbial wash was added to every plant to avoid initial differences in microbial community due to inoculation (Wagg et al., 2011). The microbial wash was obtained by suspending 20 g of dry inoculum in 400 ml of deionized water. After mixing, the liquid inoculum was filtered through a Whatman Grade 41 ashless filter paper (12.5 cm diameter, nominal retention: 20-25 µm, Cat. No. 1441 125, Cytiva), and a few drops were inspected under a microscope to ensure the absence of AMF spores. Afterwards, 10 ml of microbial wash were transferred to each seed before sowing. All pots were fertilized with nitrogen, phosphorous and potassium (NPK; 96 – 10 – 39.5 kg ha^{-1}) by adding ammonium nitrate (NH_4NO_3), triple super phosphate (TSP; 45 % P_2O_5) and potassium sulphate (K_2SO_4). The N fertilization amount was similar to that used in Ven et al. (2019), whereas P and K application amounts were halved to avoid overfertilization in combination with the added silicates. To prevent severe drought stress during dry spells, mesocosms were irrigated with rainwater collected in underground tanks. All mesocosms received the same amount of water (285 mm; cumulative over the experimental period).

One mesh bag (13 cm x 3 cm x 2 cm) with a mesh size of 30 µm, which is permeable to AMF hyphae but excludes roots, was buried vertically in each mesocosm at a depth of 0-10 cm. The mesh bags were filled with white sand that was preheated in the oven at 550 °C for 5 h to remove organic matter.

During the experiment, several plants were infected with corn smut, a disease caused by the pathogenic fungus *Ustilago maydis* (DC., 1842). The fungus forms tumours on the aerial parts of its host plant (Matei and Doehlemann, 2016) and can significantly decrease maize yield (Clough et al., 2011). Whenever a plant was infected and a tumour was observed, the tumour was removed from the plant. Fresh weight was determined, whereafter the tumour was dried in the oven at 70 °C for 48 h and its dry weight was recorded. Corn smut weight did not differ among the treatments (Table S2).

2.2 Soil chemical fertility and pore water measurements

From 1 June 2022, soil pore water samples were collected every two weeks using rhizon samplers (Rhizon Flex, Rhizosphere Research Products B.V.) installed vertically at 0-10 cm depth in each mesocosm. Pore water analyses included alkalinity, pH, and concentrations of DIC, aluminium (Al), nickel (Ni), and zinc (Zn). Pore water calcium (Ca), iron (Fe), potassium (K), magnesium (Mg), sodium (Na), ammonium-nitrogen (NH_4^+-N), nitrate-nitrogen (NO_3^--N), phosphate-

phosphorus (PO_4^{3-}-P), silicon (Si), sulphate (SO_4^{2-}), copper (Cu) and manganese (Mn) concentrations were also quantified and are reported in Fig. S2-3. Soil pore water pH was measured with a flat membrane electrode (6.0256.100, Metrohm) connected to a 914 pH/Conductometer (2.914.0020, Metrohm). DIC was measured on three technical replicates with a TOC analyser (Formacs^{TM} HT Series, Skalar) using deionized water as blank and sodium carbonate (EMSURE, Supelco) as standard; whereas alkalinity, NH_4^+-N, NO_3^- -N, SO_4^{2-} and PO_4^{3-}-P were measured on three technical replicates by a continuous flow analyser (SAN++® Advanced Series, Skalar) using sodium carbonate (Certipur, Merck Group) and standard NH_4^+, NO_3^-, PO_4^{3-} and SO_4^{2-} solutions (Certipur, Supelco) as quality controls respectively. DIC, NH_4^+-N, NO_3^--N, PO_4^{3-}-P and SO_4^{2-} analyses were conducted in-house on samples filtered through a disposable 0.45 µm PET-45/25 membrane filter (CHROMAFIL, Macherey-Nagel). Elemental analyses were performed by inductively coupled plasma-optical emission spectrometry (ICP-OES, DSOI SpectroGreen, SPECTRO) in the Helmholtz Laboratory for the Geochemistry of the Earth Surface (HELGES) on samples filtered through a disposable 0.2 µm PET-20/25 membrane filter (CHROMAFIL, Macherey-Nagel) and acidified with 10 ml 65% nitric acid (HNO_3), using international water reference material SLRS-6 (NRC-CNRC) as quality control. Alkalinity measurements were carried out in-house on unfiltered samples.

Measurements of soil chemical fertility (here defined as soil pH, CEC and base saturation) were performed on soil samples collected before basalt application and on topsoil samples (0-20 cm) collected at the end of the experiment (12 September 2022). Topsoil pH was measured by collecting, pooling and air-drying three subsamples per mesocosm. Subsequently, 4 g of soil was dissolved in 10 ml deionized water (soil : water = 1:2.5) and shaken before pH measurement. Soil potential CEC and base saturation were determined by 1 M ammonium acetate (NH_4OAc) displacement at pH 7.0 using ICP-OES (iCAP6300 Duo, Thermo Fisher Scientific; Brown, 1943).

2.3 Sequential extractions of soil cations

Sequential extraction techniques are designed to quantify elements in different soil fractions (Tessier et al., 1979). These are valuable for calculating weathering rates of the silicate minerals (Niron et al., 2024; Vienne et al., 2024) as well as to quantify cations available for plant uptake (i.e., in the soil exchangeable complex). For this, soil samples were collected at the beginning of the experiment (day 9 after basalt amendment) at a depth of 0-20 cm (sampling deeper soil layers was not possible as it would entail destructive sampling). At the end of the experiment (day 113), soil samples were taken at three depth intervals (thus defining three soil layers: 0-20 cm, 20-40 cm, and 40-60 cm) and subsequently air-dried.

Sequential extractions were performed using protocols adapted from Tessier et al. (1979) and Uhlig and Von Blanckenburg (2019). In a four-step process, Al, Ca, Cr, Fe, K, Mg, Na, Ni, Si, and Zn were extracted from four soil pools, i.e., the exchangeable, carbonate, reducible and oxidizable pools. Cations that remained in the soil after the extraction process are considered to be part of the primary or secondary minerals' structure, and thus unlikely to be released under typical soil conditions (Tessier et al., 1979). The concentrations of Al, Ca, Cr, Fe, K, Mg, Na, Ni, Si, and Zn for each extraction step

were then quantified in the Helmholtz Laboratory for the Geochemistry of the Earth Surface (HELGES) on three technical replicates by ICP-OES (DSOI Spectrogreen, SPECTRO), using international water reference material SLRS-6 (NRC-CNRC) as quality control. In order to exclude the cations extracted from the initial soil and un-weathered basalt, and investigate the effect of basalt and AMF on the cations in the various soil fractions, soil cation concentrations at the start of the experiment were subtracted from the concentrations measured at the end of the experiment. In the main text only cation concentrations in the exchangeable fraction are reported and widely discussed. These are cations adsorbed onto the soil's exchangeable complex, and are therefore relevant for soil fertility, plant uptake and growth. Results from reducible and oxidizable pools are reported in the supplements (Fig. S4-5; Table S3-4) and are only briefly discussed in the main text, as they provide indication on clay-sized mineral and stable organic C formation respectively.

2.4 Weathering rates calculations

Weathering rates were calculated based on the major cations (Ca, Mg, Na, K) released from the applied basalt as in Steinwidder et al. (2025). These cations can follow several paths: they either leach out of the soil, are taken up by plants, or remain within the soil system. During the experiment, high temperatures (mean summer temperature = 19.6 °C, compared to the 17.9 °C average between 1991 and 2020; Royal Meteorological Institute, 2022) were registered, and leaching occurred only at the beginning of the experiment and in minimal volumes (mean ± SE = 0.7 ± 0.1 l; Table S5), as most of the water in the mesocosms was lost through evapotranspiration driven by plant uptake and atmospheric evaporative demand. The leaching loss of cations was thus negligible and only the cations accumulating in plant biomass and soil pools were used for the weathering rate calculations.

To determine the amount of each cation released from the applied basalt and taken up by plants (ΔCat_{plant}), leaf cation concentrations in the C-AMF treatment ($Cat_{C\text{-}AMF(leaf)}$; see Sect. 2.5 for method) were subtracted from cation concentrations in basalt-applied treatments ($Cat_{treatment(leaf)}$; Eq. (1)). Average leaf cation concentration was used to calculate the increase in mol charge equivalents with basalt application compared to C-AMF treatment.

$$\Delta Cat_{plant} = Cat_{treatment\ (leaf)} - Cat_{C-AMF\ (leaf)} \quad \text{Equation (1)}$$

In order to determine the amount of each cation released into the soil from the weathering of the applied basalt over the experimental duration (ΔCat_{soil}), initial (day 9) cation concentrations in each sequentially extracted pool i (Cat_{day9i}) were subtracted from the final cation concentrations extracted at the experiment's conclusion ($Cat_{day113i}$; day 113; Eq. (2)).

$$\Delta Cat_{released_treatment_i} = Cat_{day113_i} - Cat_{day9_i} \quad \text{Equation (2)}$$

As the extraction process also extracts primary minerals from un-weathered basalt, this approach accounts for the contribution of the un-weathered basalt to the extracted cations pool by subtracting the initial (mostly un-weathered) soil + basalt mixture from the final concentrations. Because no soil samples were collected immediately after amendment (at day 0), samples obtained at day 9 were used as the initial soil + basalt mixture. As weathering rates are highest immediately after rock application, this approach likely underestimates the true weathering rates. Nevertheless, the day 9 measurements still provide an appropriate baseline for testing our central hypothesis, namely whether AMF enhance basalt weathering rates. Although some weathering occurred before the first sampling event (Fig. S6), AMF-driven weathering is unlikely to have contributed substantially during this period because fungal hyphae require time to establish. This interpretation is supported by the pore water DIC dynamics (Fig. 3), which indicate that AMF activity increased progressively throughout the experiment rather than immediately after inoculation. Consequently, while the use of day 9 samples likely results in conservative estimates of absolute weathering rates, it does not bias our assessment of the relative effect of AMF on weathering.

For the 0-20 cm layer, initial (day 9) cation concentrations were subtracted from the final concentrations. For the deeper layers, where no basalt was incorporated, initial cation concentrations (Cat_{day9i}) were assumed to be equivalent to initial concentrations in the top layer of the control treatment without basalt (C-AMF). Any cation increase observed in the lower layers was therefore attributed to weathering products, as un-weathered basalt was absent in these layers. This calculation assumes that cation migration to the deeper soil layers occurs exclusively as a result of weathering.

Finally, in order to account for potential changes over time in the soil due to plant uptake and/or inclusion of cations within clays, the increases in cation concentration in the basalt treatments for each sequentially extracted soil pool i (ΔCat_{soili}) were expressed relative to the C-AMF treatment ($\Delta Cat_{released_C\text{-}AMFi}$; Eq. (3)). Weathering rates (Wr; expressed as $\log_{10}$ (mol charge equivalents m^{-2} s^{-1})) were then calculated as in Steinwidder et al. (2025; Eq. (4)):

$$\Delta Cat_{soil_i} = \Delta Cat_{released_treatment_i} - \Delta Cat_{released_C-AMF_i} \quad \text{Equation (3)}$$

$$Wr = log_{10}\left(\frac{2\times(\Delta Ca_i+\Delta Mg_i)+(\Delta Na_i+\Delta K_i)}{time \times application\ amount \times SSA}\right) \quad \text{Equation (4)}$$

Where ΔCa_i, ΔMg_i, ΔNa_i, and ΔK_i are the concentration changes in each soil fraction (i.e., exchangeable, carbonate, reducible and oxidizable pools) and plant pool i calculated as mentioned above (i.e., ΔCat_{soili} and ΔCat_{plant}), time is the experimental duration in seconds, application amount is 980 g mesocosm^{-1} (equivalent to 50 ton ha^{-1}) and SSA is the specific surface area of the applied basalt, with a value of 6.283 m^2 g^{-1} (see Sect. 2.1).

2.5 Plant measurements

Plants were harvested on 12 September 2022. The three top leaves of each plant were sampled for further analysis, whereafter the aboveground biomass was harvested and separated into stems, leaves, tassels and corn. Aboveground biomass was then dried at 70 °C for 48 h and the dry weight of each organ was determined. After harvesting the aboveground biomass, roots were sampled from the topsoil (0-20 cm), middle soil (20-40 cm) and bottom soil (40-60 cm) layers to estimate the root biomass within each mesocosm. For each layer, two 100-cm^3 cores were taken directly beneath each plant and one between the two plants. The roots were then washed using a 1 mm mesh sieve, after which they were dried at 70 °C for 48 h and weighed. Root biomass estimates assumed that cores beneath the plants represented root growth in half of the mesocosm, while cores between the plants reflected the other half (as in Ven et al., 2020). Before analysis, the three top leaves (hereafter referred to as leaves), stems, tassels, corn kernels and roots were ground using a centrifugal mill (ZM 200, Retsch GmbH) with a 0.25 mm mesh size sieve.

Plant samples were analysed for nutrients (C, Ca, Fe, K, N, Mg, P) and heavy metals (Al, Cd, Cr, Ni, Pb, V and Zn). Dried, homogenized plant material was subjected to acid digestion with 70 % HNO_3 at 60 °C for 30 minutes, followed by the addition of 30 % hydrogen peroxide (H_2O_2) and further heating at 120 °C for 90 minutes. After cooling and filtering, elemental concentrations were measured by ICP-OES (Thermo Scientific, iCAP 6300 Duo). Quantification was based on multi-element calibration standards (CPAChem), with yttrium (Merck) used as an internal standard. A certified reference material (Hay Powder BCR129, CPAChem) was processed alongside the samples using identical digestion procedures. Quality control checks were conducted every 20 measurements to ensure analytical precision and accuracy. Plant Ni, Cr and Mg results are reported in the main text, while concentrations of all other elements are reported in the supplements (Fig. S7). Biogenic Si was determined by digestion of a 0.03 g plant sample with 25 ml 0.5 M sodium hydroxide (NaOH) and then analysed with a continuous flow analyser (SAN++® Advanced Series, Skalar) following Demaster (1981); and Saccone et al. (2007).

2.6 AMF measurements

To determine plant root colonization by AMF, plant roots were first cleared and then stained using a non-vital staining technique (Vierheilig et al., 2005). Washed roots were cleared by placing them in an Erlenmeyer flask containing a 5 % potassium hydroxide (KOH) solution which was then set in a warm water bath at 90 °C for 8 minutes. Hereafter, the roots were rinsed and stained with 10 % Sheaffer Black ink in 10 % acetic acid by placing them in a warm water bath at 90 °C for 10 minutes. To remove excess ink, the roots were immersed in lactoglycerol (1:1:1 lactic acid : glycerol : deionized water) and stored in an Eppendorf tube with lactoglycerol overnight at 4 °C (Fig. S8). The proportion of roots colonized with mycorrhizal fungi was then quantified by counting arbuscules, vesicles and hyphae using the gridline intersection method (Giovannetti and Mosse, 2006).

During the harvest on 12 September 2022, the mesh bags were removed from the mesocosms and stored frozen until further analysis. Hyphal length of the mycorrhizae was subsequently determined according to Rillig et al. (1999) with adaptations as in Ven et al. (2019).

2.7 Data analysis

All statistical analyses were performed in R using packages nlme, lmerTest and dunn.test (Kuznetsova et al., 2017; Pinheiro et al., 2007; R Core Team, 2024; v4.3.1; Dinno, 2024). The level of significance for all analyses was set at $p < 0.05$. A factorial analysis of variance (ANOVA) was used to investigate the effects of basalt application, AMF inoculation, and their interaction on soil pH, CEC, base saturation, exchangeable cation concentration in each soil layer and weathering rates. If normality or homoscedasticity of the model residuals were not met after log- or square-root transformation, the non-parametric Kruskal-Wallis test was used with treatment (C-AMF, C+AMF, B-AMF and B+AMF) as explanatory variable. A post-hoc test (Tukey's honestly significant difference test or Dunn's multiple comparison test for parametric and non-parametric analyses respectively) was conducted to explore significant differences among treatments.
When cation concentrations in soil were below the detection limit (=bd; Table S6-7), the concentrations were set to zero to allow further statistical analyses. In some cases, the presence of the cation was detectable, but the very low concentration did not allow an accurate quantification. For these measurements, half of the limit of quantification was used for statistical analyses.

To quantify treatment effects on variables with repeated measurements over time, i.e., pore water pH, DIC, alkalinity, and nutrient and heavy metal concentrations in the pore water, a linear mixed model was employed. Basalt application, AMF, time (days after basalt application), and their interactions were included as fixed effects, and mesocosm was included as a random effect term. To assess whether the presence of galls from corn smut was affected by basalt, AMF or their interaction, a generalized linear model was used with the binomial family, as appropriate when modelling binary response variables.

The data and model code in support of our findings are openly available in Zenodo at https://doi.org/10.5281/zenodo.16813184 (Boito, 2025).

3 Results

3.1 Basalt improved soil chemical fertility, but did not affect most pore water nutrients

At the end of the experiment, basalt significantly increased soil pH (+0.71 ± 0.14), CEC (+0.43 ± 0.18 meq 100 g^{-1}), and base saturation (+13.6 ± 3.5 %; Fig. 2). The influence of basalt on soil pH, CEC, and base saturation was not affected by AMF. Similarly, pore water pH (+0.41 ± 0.12) and alkalinity (+0.26 ± 0.08 meq l^{-1}) also increased with basalt, again without influence of AMF (Fig. 3). All reported values represent mean basalt effects ± SE. Concerning DIC, our data showed

significant two- and three-way interactions between basalt and time and between basalt, AMF, and time respectively. Without AMF, basalt increased pore water DIC concentrations between the start and the end of the experiment by 2.35 mg l^{-1}. This effect became more pronounced in the presence of AMF: DIC concentrations in the B+AMF treatment increased by 9.6 mg l^{-1} more than in the control over the same period (day 10-102; Fig. 3).

On the other hand, concentrations of plant-available nutrients in the pore water were generally not significantly affected by basalt application nor AMF presence, with the exception of basalt-driven increases in Mg and Na in the middle of the growing season (Fig. S2). Pore water Mg also showed a significant three-way interaction effect of basalt, AMF and time, with AMF reinforcing the positive effect of basalt.

Concerning heavy metals, Cr in the pore water was below the limit of quantification (<0.02 mg l^{-1} for pore water concentrations) in all samples and for Ni, 32.3 % of the samples were below the limit of quantification. Nonetheless, basalt increased Ni concentration until around day 75 (Fig. 4). A significant time x basalt interaction was found on Zn concentrations in the pore water, although without a clear trend. Pore water Al decreased with basalt amendment, and AMF presence decreased pore water Al but only in control mesocosms (significant basalt x AMF interaction).

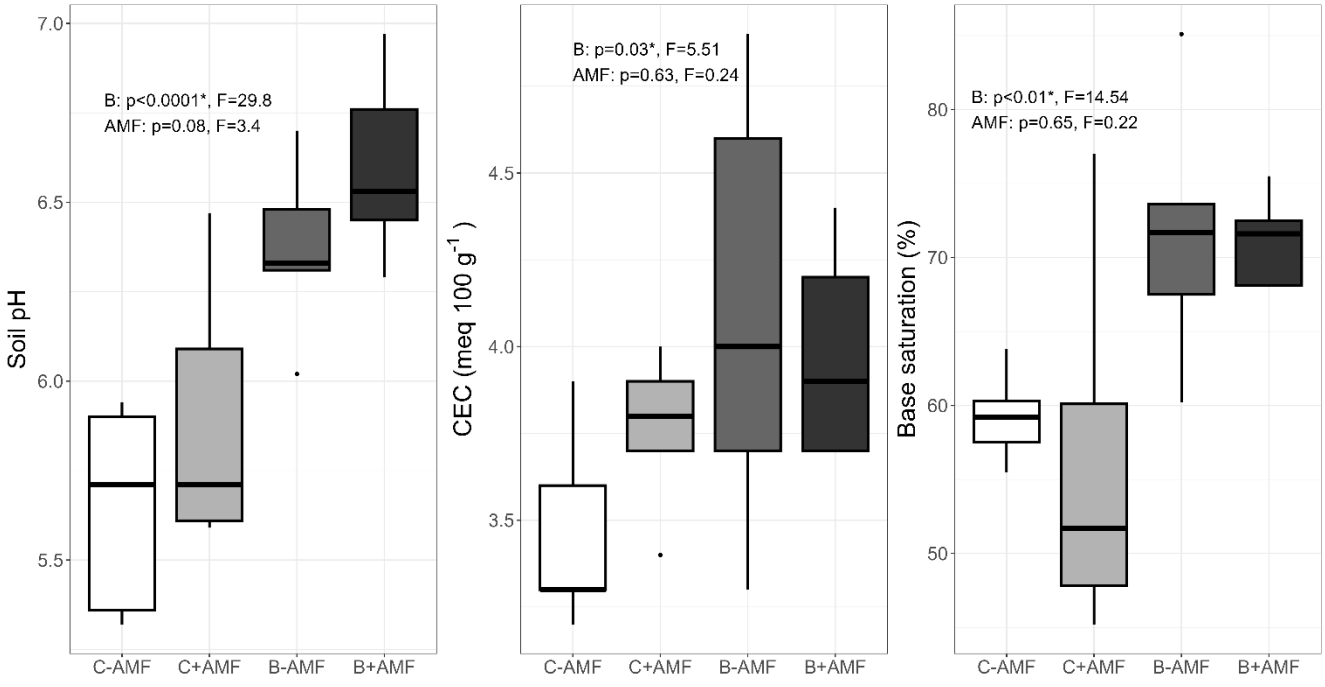


Figure 2: Soil pH (a), cation exchange capacity (CEC, b) and base saturation (c) of the four treatments (C-AMF = control without AMF, C+AMF = control with AMF, B-AMF = basalt without AMF, B+AMF = basalt with AMF) at the end of the experiment. Boxes represent the interquartile range (25th-75th percentile), horizontal lines indicate the median, and whiskers extend to the most extreme data points within 1.5x of the interquartile range. Points outside this range are plotted as outliers. p- and F-values from an ANOVA analysis with pH, CEC or base saturation as response variables and basalt (B), AMF and their interaction as covariables are shown. Interactions were not significant and were excluded from the model. Statistical significance is indicated by an asterisk (*).

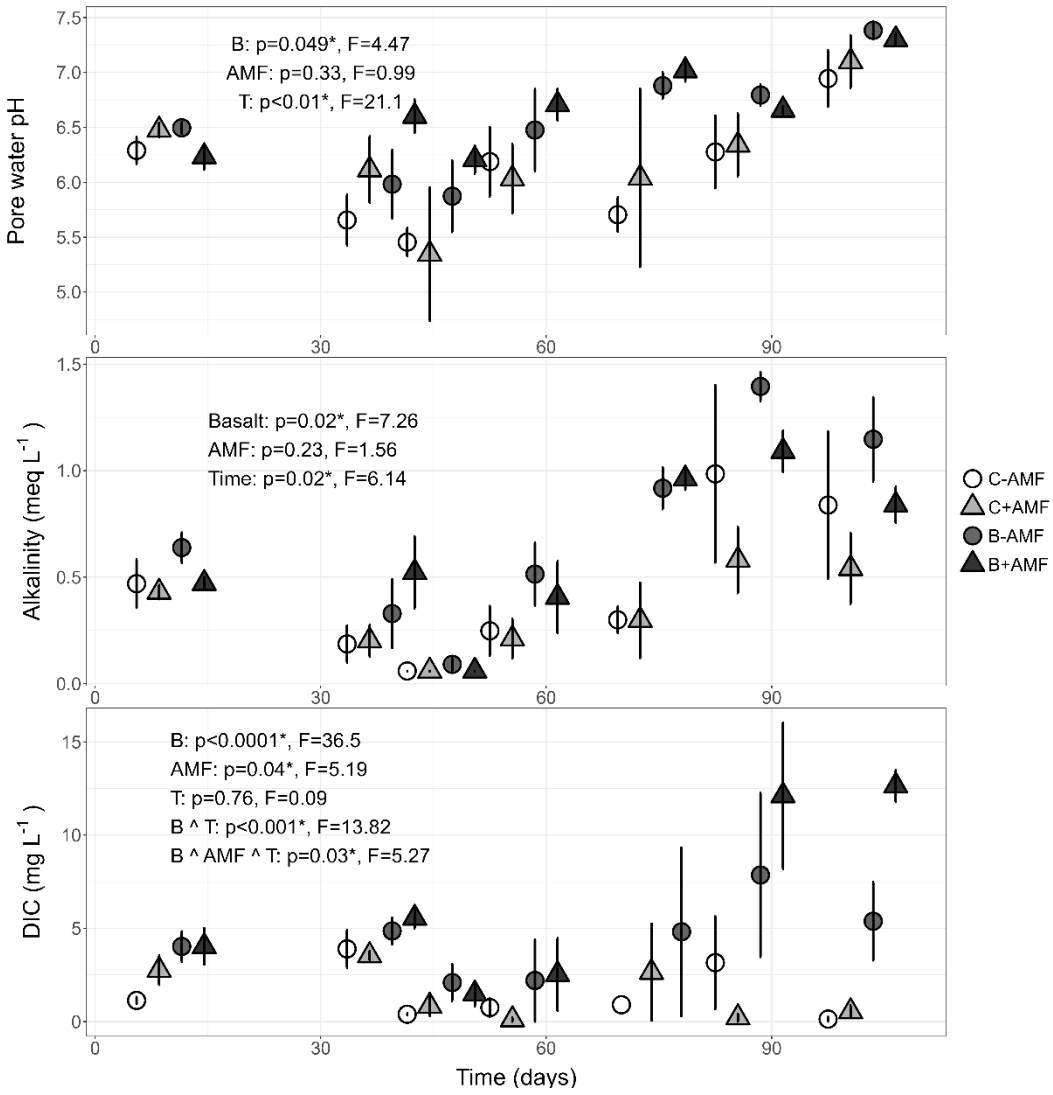


Figure 3: Mean pH (a), total alkalinity (b) and dissolved inorganic carbon (DIC, c) in the soil pore water during the experiment for the four treatments (C-AMF = control without AMF, C+AMF = control with AMF, B-AMF = basalt without AMF, B+AMF = basalt with AMF). Error bars represent the standard error on the mean. p- and F-values from a linear regression analysis with pH, total alkalinity or DIC as response variable and basalt (B), AMF, time (T), and their relevant interactions as covariables are shown. When interactions were not significant, they were excluded from the model and are not shown here. Interactions are indicated by carets (^), while significant relationships by an asterisk (*).

3.1.1 Basalt increased exchangeable Ca, Mg and Na, while it decreased exchangeable Zn

Basalt application increased exchangeable Ca and Mg in the 0-20 (Ca = +87.5 ± 37.7; Mg = +11.5 ± 5.9 mg kg soil^{-1}) and 20-40 (Ca = +72.6 ± 11.3; Mg = +36.3 ± 2.0 mg kg soil^{-1}) cm layers but not in the 40-60 cm layer (Fig. 5; Table S3-4). Additionally, basalt increased exchangeable Na in the 20-40 cm layer (+20.3 ± 2.0 mg kg soil^{-1}), and in the 0-20 cm layer a post-hoc pairwise comparison revealed a significant Na increase between C-AMF and B+AMF treatments (+21.9 mg kg soil^{-}

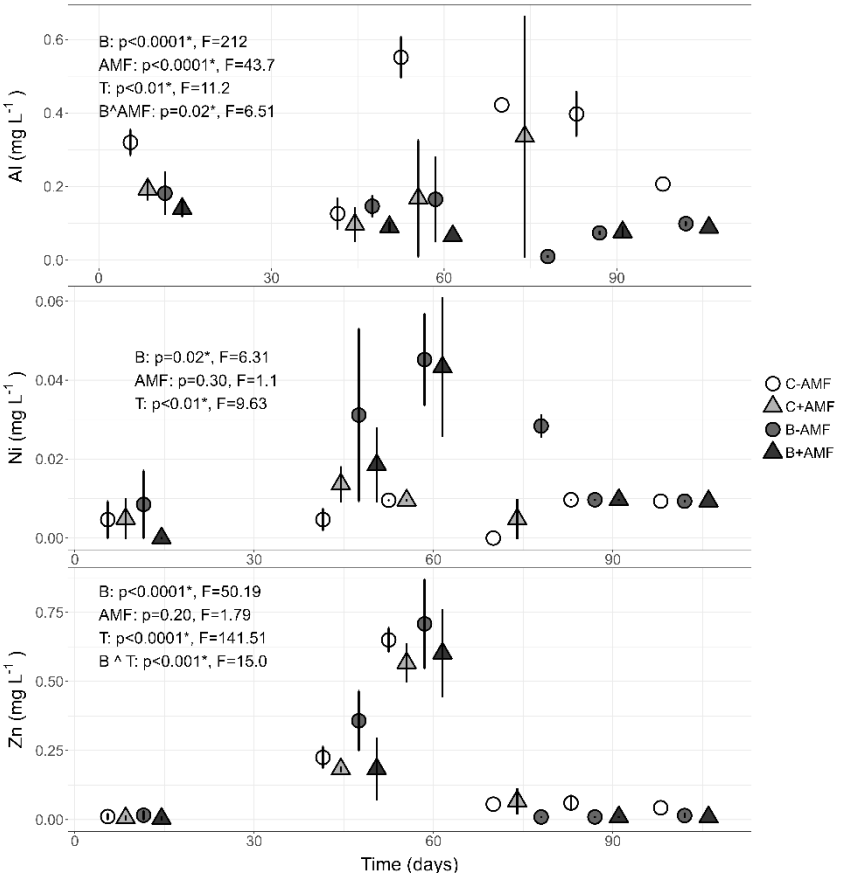


Figure 4: Pore water Al (a), Ni (b) and Zn (c) concentrations during the experiment for the four treatments (C-AMF = control without AMF, C+AMF = control with AMF, B-AMF = basalt without AMF, B+AMF = basalt with AMF). Error bars represent the standard error on the mean. p- and F-values are shown from a linear regression analysis with heavy metal concentration as response variable, and basalt (B), AMF, time (T), and their relevant interactions as covariables. When interactions were not statistically significant, they were excluded from the model and not shown here. Interactions are indicated by carets (^), while significant relationships by an asterisk (*).

^{1}). On the other hand, exchangeable K, Fe and Si concentrations were not affected by basalt application (Fig. 5; Table S3). Concentrations of exchangeable Ni and Cr were below the limit of quantification in all layers, and the same was true for Al in the 40-60 cm layer (Table S6), hence precluding formal statistical analysis of these elements in the exchangeable pool of those layers. This was not the case for exchangeable Al in the 0-20 and 20-40 cm layers, which was not affected by basalt application, and exchangeable Zn, which decreased in the 0-20 and 20-40 cm layers (-0.3 ± 0.1 and -0.6 ± 0.1 mg kg soil^{-1} respectively; Fig. 6; Table S3-4). AMF did not affect cation concentrations in the sequentially extracted soil pools.

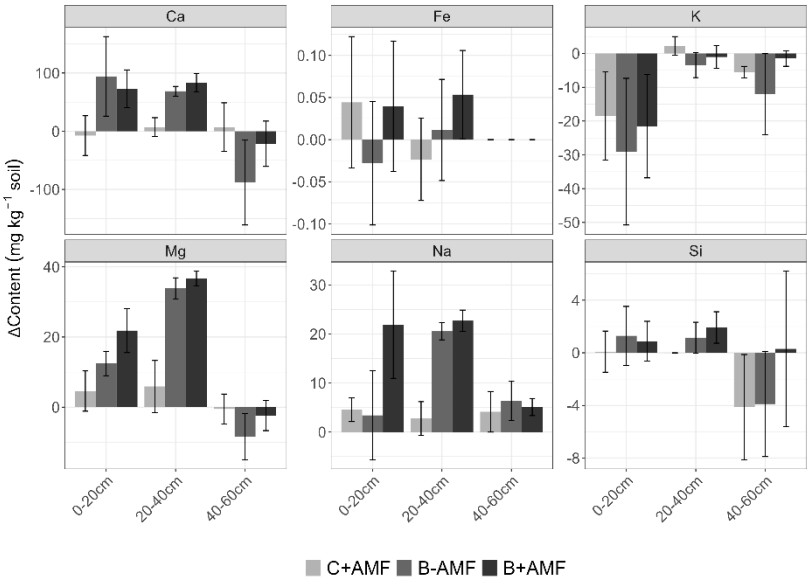


Figure 5: Mean Δ soil nutrient contents (Ca, Fe, K, Mg, Na and Si) for three treatments (C+AMF = control with AMF, B-AMF = basalt without AMF, B+AMF = basalt with AMF) at the end of the growing season. Error bars represent the standard error on the mean. Nutrient contents are shown as the difference between the start and the end of the growing season, and are expressed relative to the control treatment (C-AMF = control without AMF). Soils were divided into three sampling depths (0-20 cm, 20-40 cm, 40-60 cm) for which nutrient concentrations were measured in the exchangeable fraction with the sequential extraction method after Tessier et al. (1979). p- and F-values from an ANOVA analysis with nutrient concentration as response variables, and basalt, AMF and their interaction as covariables are presented in Table S3.

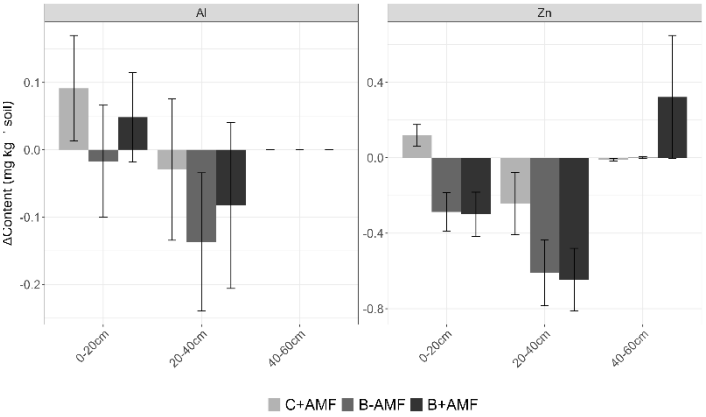


Figure 6: Mean Δ soil heavy metal content (Al and Zn) for three treatments (B-AMF = basalt without AMF, B+AMF = basalt with AMF, C+AMF = control with AMF) at the end of the growing season. Error bars represent the standard error on the mean. Heavy metal contents are shown as the difference between the start and end of the growing season, and are expressed relative to the control treatment (C-AMF; control without AMF). Soils were divided into three sampling depths (0-20 cm, 20-40 cm, 40-60 cm) for which heavy metal concentration in the exchangeable fraction was measured with the sequential extraction method after Tessier et al. (1979). p- and F-values from an ANOVA analysis with nutrient concentration as response variables, and basalt, AMF and their interaction as covariables are presented in Table S3.

365

3.2 AMF did not affect basalt weathering rates

Similarly, basalt weathering rates were not affected by AMF presence (Fig. 7), with rate constants corresponding to -9.97 ± 0.04 and -10.01 ± 0.05 $\log_{10}$(mol charge equivalents m^{-2} s^{-1}) for
370 treatments with and without AMF, respectively. This corresponds to the weathering of 37.5 % ± 3.7 and 33.2 % ± 4.0 of Ca-, Mg-, Na- and K-bearing minerals in the applied basalt (including both crystalline and amorphous phases), in the presence and absence of AMF respectively, over the 113-day experimental period.

375 When comparing Mg, Ca, Na and K changes in soil pools with changes in plant pools, it emerged that the greatest contribution to the increase in released cations was in the soil phase, with a total increase in the soil about two orders of magnitude greater than in the plants (Table S8).

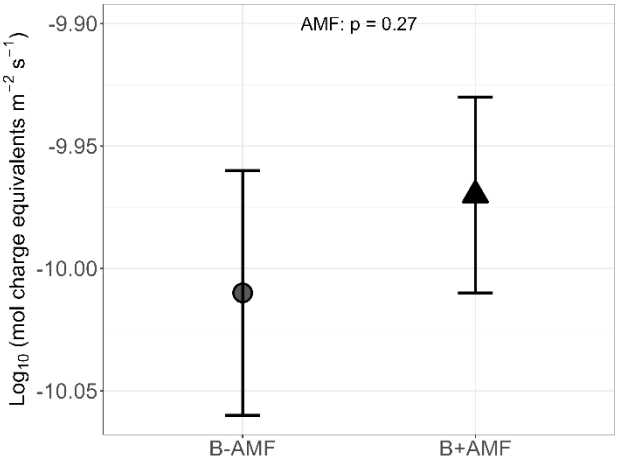


Figure 7: Mean basalt weathering rates for the basalt treatments calculated as the increase in base cations (Ca, Mg, K, Na) in the soil phase and in the plants between the start and the end of the experiment, and corrected for the control soil (C-AMF = control without AMF). Error bars represent the standard errors on the mean. p- and t-values from a two-sample t-test are presented.

380

3.3 Limited basalt and AMF effects on crop growth, biomass and quality

Generally, plant growth parameters were not affected by basalt or AMF, including measurements of individual plant organs (Fig. S9-10). In addition, no effect of basalt on AMF hyphal length and root colonization was found (Fig. 1). Corn smut presence did not differ among treatments, nor did the weight of the galls (Table S2). Elemental concentrations (Ca, Fe, Mg,

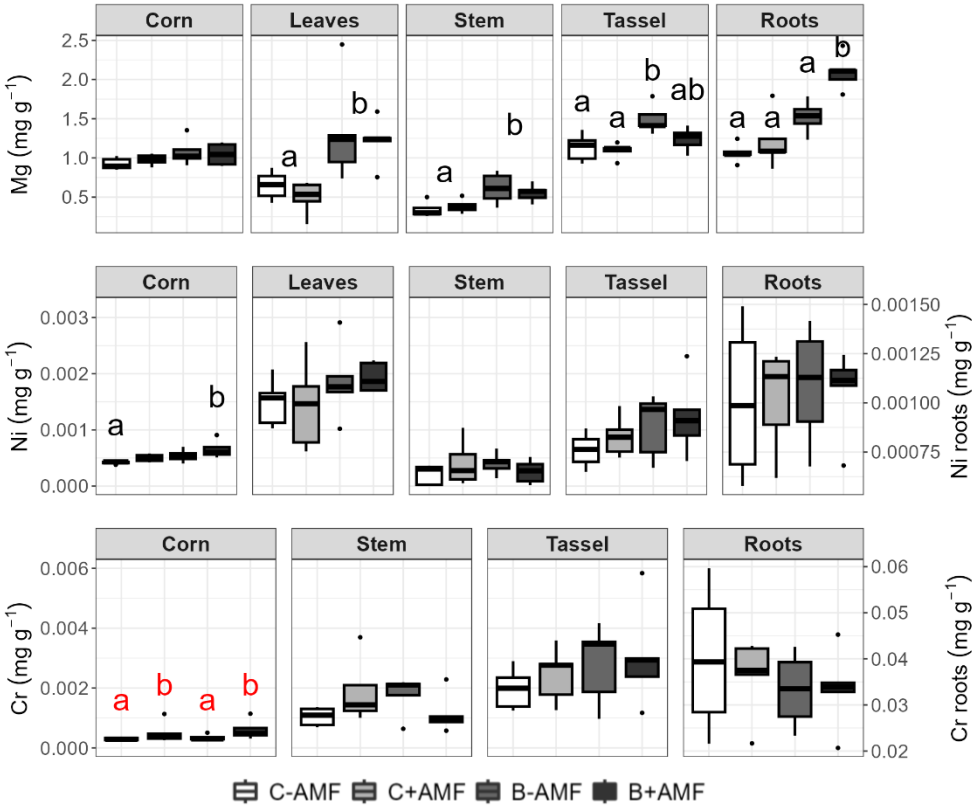


Figure 8: Concentration of Mg (a), Ni (b) and Cr (c) in the corn, leaves, stem, tassel, and roots for the four treatments (B-AMF = basalt without AMF, B+AMF = basalt with AMF, C-AMF = control without AMF, C+AMF = control with AMF) at the end of the experiment. Boxes represent the interquartile range (25th-75th percentile), horizontal lines indicate the median, and whiskers extend to the most extreme data points within 1.5x of the interquartile range. Points outside this range are plotted as outliers. Note that for Cr and Ni, the primary axis shows the concentration in the corn, leaves, stems, and tassels while the secondary axis shows the concentration in the roots. p- and F-values are shown in Table S9. Significant differences are indicated with a different letter, while a similar letter means no differences between those treatments. Black letters indicate basalt effects, while red letter indicate AMF effects. If no letters are shown for a combination of plant part and element, this means that there was no significant influence of basalt or AMF.

385 K, Si, P) in plant parts were typically not affected by basalt or AMF application, with a few exceptions. A notable exception was Mg, whose concentration in plant organs was generally higher with basalt application, save for corn Mg where no basalt effect was found, and tassel Mg in which a post-hoc comparison revealed an increase with basalt only in absence of AMF (B-AMF treatment compared to C-AMF and C+AMF; Fig. 8; Table S9). Despite this, no significant AMF x basalt interaction effect on tassel Mg emerged. On the other hand, in contrast with other elements in other plant organs, a

borderline significant (p=0.08) basalt x AMF interaction effect was found on root Mg concentrations, which only increased with basalt when AMF were present. Moreover, basalt decreased leaf K, whereas AMF decreased leaf P. Finally, stem and tassel Si concentrations increased with basalt application (Fig. S7; Table S9).

Leaf Cr concentrations were all below the limit of quantification (<0.0002 mg g^{-1}). Therefore, statistical analyses could not be conducted for leaf Cr. Basalt application did not affect Al, Cr and Zn concentrations in the various plant organs (Fig. 8; Fig. S7; Table S9). In contrast, corn Ni concentrations were significantly higher with basalt and AMF, but a post-hoc pairwise comparison revealed that only the C-AMF – B+AMF difference was significant (Fig. 8; Table S9). Finally, AMF increased corn Cr (Fig. 8; Table S9).

4 Discussion

4.1 Weathering rates and proxies

In contrast with our hypothesis, AMF did not significantly increase basalt weathering rates. This limited response likely reflects the relatively nutrient-rich conditions of the experiment. The soil used was relatively fertile and only moderately acidic (initial pH = 5.6), and all mesocosms received NPK fertilizer (96 – 10 – 39.5 kg ha^{-1}). Although P and K application rates were slightly below Flemish recommendations (Departement Landbouw & Visserij, 2016; Vlaamse Land Maatschappij, 2026), no visible symptoms of nutrient deficiency were observed in the plants. Hence, P availability was likely sufficient, reducing the incentive for AMF-mediated P acquisition. Under such conditions, the potential for AMF to stimulate mineral dissolution through biological weathering could be reduced. These findings suggest that AMF-induced enhancement of silicate weathering may be limited in fertilized soils where plant P demand is largely satisfied.

Because the first soil samples were collected nine days after basalt application, the weathering rates estimated in our experiment likely underestimate absolute weathering rates, as mineral dissolution is generally fastest shortly after amendment. However, this limitation is unlikely to affect the comparison between AMF treatments: AMF colonization develops gradually following inoculation, making a substantial AMF contribution to weathering during the first nine days unlikely. Thus, while the absence of day-0 measurements introduces uncertainty into the absolute weathering-rate estimates, it should not bias our conclusion that AMF did not measurably enhance basalt weathering.

Nevertheless, the weathering rates estimated through cation mass balance in our experiment (−9.97 ± 0.04 and −10.01 ± 0.05 $\log_{10}$ mol charge equivalents m^{-2} s^{-1} in the presence and absence of AMF, respectively) were more than one order of magnitude higher than weathering rates based on cation tracing previously reported by comparable mesocosm experiments. In a similar experiment, Steinwidder et al. (2025) reported weathering rates of −11.15 ± 0.16 $\log_{10}$ mol charge equivalents

m^{-2} s^{-1} (14-15 times slower than in our experiment) using the same methodology, 15 months after application of 50 ton ha^{-1} of the same basalt to the same soil, albeit unpasteurized. Similarly, Vienne et al. (2024) reported a mean weathering rate of -11.65 ± 0.09 $\log_{10}$ mol charge equivalents m^{-2} s^{-1} (44-48 times slower than in our experiment) following application of 100 ton ha^{-1} of basalt over 137 days. The comparatively high weathering rates observed here may be related to the pasteurization process: heating the soil at 80 °C for four hours likely generated substantial microbial necromass and increased dissolved organic carbon (DOC) concentrations. In particular, low-molecular weight organic acids, which are an important component of DOC, have been shown to sustain far-from-equilibrium conditions that drive rapid elemental loss, and potentially weathering rates as well (Perez-Fodich and Derry, 2019). Indeed, pore water DOC concentrations in pasteurized mesocosms were on average 158 % higher ($+22.8 \pm 3.5$ mg l^{-1}) than those observed in comparable unpasteurized systems (Fig. S11), consistent with enhanced DOC availability contributing to the higher weathering rates observed here.

Despite these comparatively high dissolution rates, weathering rates estimated from cation mass balance remained approximately three orders of magnitude lower than those predicted from laboratory-derived dissolution kinetics (-7.0 ± 0.08 $\log_{10}$ mol charge equivalents m^{-2} s^{-1} for the amended feedstock; S1). Such discrepancy is consistent with previous observations that laboratory-derived weathering rates commonly exceed field-derived rates by one to five orders of magnitude (White and Brantley, 2003), while mesocosm experiments typically yield intermediate values (Malmström et al., 2000). Such differences highlight the strong influence of experimental scale on estimated weathering rates. However, variability in weathering rates cannot be attributed to experimental scale alone, as mineral dissolution rates are also strongly affected by feedstock properties and environmental conditions (Palandri and Kharaka, 2004). Even among basalt feedstocks, dissolution rates may vary by up to a factor six due to differences in mineralogy, glass content, particle size distribution, and elemental composition (Lewis et al., 2021). Likewise, environmental conditions such as soil type, temperature and water availability can substantially influence weathering dynamics (Dupla, 2025). Consequently, weathering rates reported across studies should be compared with caution, particularly when experiments differ simultaneously in scale, feedstock composition and environmental conditions.

4.1.1 Reconciling contrasting weathering proxies

Pore water pH, alkalinity and Mg increased with basalt application, with no AMF effect, whereas pore water DIC showed a significant basalt x AMF x time interaction (Fig. 3; Fig. S2). The observed increase in pore water DIC with basalt application was reinforced by AMF towards the end of the experiment, as the fungal hyphae developed. The observed increase in pore water DIC with AMF might suggest that AMF increased basalt weathering rates. However, other weathering proxies such as pore water pH, alkalinity, Ca and Mg did not show similar patterns. This discrepancy between DIC and the other weathering indicators may be due to different reasons.

While silicate weathering is expected to increase DIC through (bi)carbonate production, the observed increase in DIC may also reflect elevated soil partial CO_2 pressure (pCO_2). Pore water DIC is governed by carbonate equilibria, which are sensitive to transient environmental conditions such as pore water pH and pCO_2 (Hartmann et al., 2013; Zeebe and Wolf-Gladrow, 2001). Indeed, higher pCO_2 can increase dissolved carbonic acid (H_2CO_3) and therefore DIC. As the pore water pH of the basalt-treated mesocosms in our experiment was > 6.5 in the second half of the experiment (Fig. 3), the dissolved H_2CO_3 likely predominantly speciated into (bi)carbonate ions within the soil solution, leading to elevated DIC.

A second possible explanation for the discrepancy between pore water DIC and alkalinity lies in the role of anions in alkalinity. Total alkalinity is the sum of base cation charges, minus the sum of conservative anion charges (e.g. Cl^-, SO_4^{2-}, PO_4^{3-}, NO_3^-) (Wolf-Gladrow et al., 2007). While DIC increased with AMF, other anions may have decreased, leading to a null effect of AMF on alkalinity. We did not find a decrease in pore water NO_3^-, SO_4^{2-}- and PO_4^{3-} with AMF (Fig. S2-3), but organic anions may still have contributed to the observed effect. During the middle of the growing season, basalt treatments with AMF tended to have lower DOC compared to basalt treatments without AMF (−11.9 mg l^{-1}; Fig. S11), partially supporting this hypothesis.

Finally, cation uptake may have also played a role. Plants and AMF act as a sink for cations, and a positive effect of AMF on this plant and AMF sink may have contributed to the observed decoupling between DIC and base cations. In this case, we would observe an increase in Ca and Mg stocks in the plant and/or AMF tissues. However, basalt only increased Mg stocks in plants, without an effect on Ca stocks (Fig. S12). Therefore, the plant sink hypothesis can only partially explain the observed mismatch between DIC and other weathering proxies such as pore water cations.

Although we cannot fully disentangle the divergence of different weathering proxies, the inconsistencies in their responses highlight the limitations of relying on a single proxy to assess weathering dynamics, as it may not adequately capture the complexity of the system (see also Iff et al. (2024)). According to the explicit conservative expression for total alkalinity (Wolf-Gladrow et al., 2007), DIC and alkalinity consist of distinct chemical species, thus complicating the interpretation of these weathering proxies. Therefore, our results suggest that cation accounting, rather than carbon accounting, may provide a more reliable estimate of weathering dynamics, as proposed by Bijma et al. (2025).

4.2 Basalt, but not AMF, improved soil chemical fertility measures

Basalt, but not AMF, increased soil pH, CEC and base saturation (Fig. 2). The observed increases in soil pH, CEC, and base saturation upon basalt application align with our hypothesis of basalt improving soil chemical fertility, although these did not translate into increased maize growth or biomass during the 113-day experiment. The observed increase in base saturation was attributable to an increase in soil exchangeable Ca, Mg and Na due to basalt application (Fig. S13). Indeed, during weathering of basalt, protons are consumed and cations are released. Additionally, weathering of primary minerals promotes

the formation of metal (hydr)oxides and secondary silicate phases, ultimately increasing the content of clay-sized particles in the soil and therefore CEC (Righi and Meunier, 1995). Our results corroborate previous work that observed increased soil pH and CEC upon basalt application to tropical soils (Anda et al., 2015; Conceição et al., 2022; Gillman, 1980). An increase in pH was also found in experiments conducted in using relatively younger, less cation-depleted soils upon basalt or dunite application (Rijnders et al., 2023; Rijnders et al., 2025; Skov et al., 2024; Ten Berge et al., 2012).

4.2.1 Limited AMF and basalt effects on soil nutrients

While basalt amendment increased soil CEC and pH, it generally did not affect soil nutrient concentrations, with a few exceptions. Despite an increase in exchangeable Ca and Mg, only Mg increased in the pore water as well. This might be at least partially explained by weathering kinetics: the Mg-rich mineral olivine weathers relatively quickly compared to other Ca-bearing minerals within the applied basalt, such as Ca-enriched plagioclase feldspars (Gudbrandsson et al., 2011). Nevertheless, basalt increased exchangeable Ca (Fig. 5; Fig. S13), indicating that Ca was released during weathering, as observed by Li and Dong (2013), Niron et al. (2024) and Vienne et al. (2022). Our pore water and exchangeable Ca results also indicate that, once released, Ca was rapidly adsorbed onto soil exchange sites rather than remaining in solution, consistent with adsorption lyotropic series (Strawn et al., 2019).

The observed Mg and Ca increases in the exchangeable fraction are in agreement with existing literature, as application of basalt supplies new cations that can bind to soil particles, increasing base saturation (Gillman, 1980; Gillman et al., 2001, 2002; Te Pas et al., 2023). Increases in exchangeable Ca and Mg were also reported by Buss et al. (2023), whereas in a mesocosm experiment by Niron et al. (2024), basalt application did not affect any of the measured cations (Ca, Mg, K, Na, Fe and Al) in the exchangeable fraction, thus contrasting our findings. On the other hand, in our experiment exchangeable Zn, an important micronutrient, decreased with basalt application in the two top layers, a result consistent with previous research (Buss et al., 2023; Desmalles et al., 2025). Generally, above a pH of 6 exchangeable Zn contents tend to be very low (Blume et al., 2010). Therefore, the observed increase in soil pH from 5.6 ± 0.1 to 6.4 ± 0.2 following basalt application may have contributed to the reduction in exchangeable Zn.

Our finding of increased exchangeable Mg and Ca (albeit not in all soil layers) is cautiously encouraging, given the global imperative to restore and maintain soil nutrient levels to support sustainable agricultural productivity (Un General Assembly, 2015). Indeed, the exchangeable pool consists of cations adsorbed onto soil particles that can be readily exchanged with the soil solution (Tessier et al., 1979), representing a key reservoir of nutrients, from which plant roots primarily acquire elements essential for growth (Roy and Finck, 2006). At the same time, even though basalt contains Fe, and in smaller amounts K, which are important plant nutrients, their concentration in the exchangeable and pore water pools did not increase with basalt application, stressing the need to be cautious when expecting soil nutrient replenishment co-benefits

from basalt application. Moreover, the observed decrease in exchangeable Zn underscores the need for careful evaluation of both unintended side-effects as well as potential co-benefits associated with enhanced weathering.

Finally, AMF did not significantly affect (micro)nutrient concentrations in the soil pore water nor in the soil exchangeable complex. Our results are thus in contrast with our hypotheses, as we expected increases in (micro)nutrient availability and/or uptake with AMF. This outcome may be at least partially attributed to the experimental conditions, namely the relatively fertile soil in combination with the fertilizer addition, as explored in Sect. 4.1.

4.2.2 Potential for future soil organic C stabilization and clay-sized particles formation

Most of the agriculturally relevant (micro)nutrients present in the basalt, namely Ca, Mg and Fe, increased in the reducible pool in the 20-40 cm layer. The net basalt effect amounted to +116.0 ± 9.3 mg kg^{-1} for Ca, +1200 ± 71.6 mg kg^{-1} for Mg, and +668.3 ± 109.2 mg kg^{-1} for Fe. Likewise, basalt increased oxidizable Ca and Si by 4.5 ± 0.7 mg kg^{-1} and 27.6 ± 9.5 mg kg^{-1}, respectively (Fig. S4; Table S3). The reducible and oxidizable pools comprise cations bound to metal (hydr)oxides and organic matter respectively (Tessier et al., 1979). Cations in these fractions are expected to be retained in the soil for a relatively long time, with plants able to access these nutrients only upon weathering (Niron et al., 2024; Palandri and Kharaka, 2004). Nevertheless, metal (hydr)oxide formation can ultimately increase CEC and govern SOC stabilization processes (Basile-Doelsch et al., 2015; Beerling et al., 2020; Manning et al., 2024; Totsche et al., 2017), with downstream benefits for plant growth and soil fertility, particularly in agricultural soils which are often depleted in organic matter (Rusco et al., 2001). Although the total stock of cations in the oxidizable fraction was relatively small compared to other soil pools (Fig. S4), the observed increases in Ca and Si following basalt application are consistent with pathways that may contribute to organic matter stabilization. More specifically, such processes have been linked to improved soil structure (Buss et al., 2023; Steinwidder et al., 2025) and mineral-associated organic matter (MAOM) formation (Niron et al., 2024) in EW experiments, although these properties were not directly assessed in the present study.

4.3 Limited basalt and AMF effects on crop yield and quality

In line with our soil nutrient data and contrary to our hypotheses, plant nutrient concentrations were generally not affected by basalt application or AMF presence, with the exception of Mg, which generally increased with basalt. Increased plant Mg can be directly linked with the observed increase in pore water Mg concentrations and Mg exchange capacity, leading to elevated Mg uptake. Our results are supported by research carried out on maize after basalt application (Boniao et al., 2006; Rijnders et al., 2025), and on ryegrass (Ten Berge et al., 2012) and soybean (Moretti et al., 2019) after dunite application. These consistent findings indicate that EW can help alleviate Mg deficiency, which often occurs in agricultural systems that are fertilized with N, P, and K as uptake competition between these elements and Mg arise (Guo et al., 2016). Nevertheless, our plant data shows only limited evidence for a positive effect of basalt and AMF on crop yield and quality, indicating that

the agronomic co-benefits of EW and AMF are modest under the relatively fertile conditions of this experiment (i.e., fertilized soil and only slightly acidic initial soil pH).

Furthermore, Na availability increased in both the soil exchangeable complex and the pore water, while leaf K concentration declined following basalt amendment. Although these changes were not associated with consistent negative effects on plant growth or biomass, they raise questions regarding the long-term EW consequences for plant nutrition, particularly shifts in the K:Na ratio that could ultimately constrain plant performance (Maathuis and Amtmann, 1999). Even though leaf Na concentrations were not measured in this experiment, we recognize Na-K antagonism as a potential concern over longer timescales, especially under repeated basalt applications.

Contrary to our hypothesis, basalt amendment did not affect AMF root colonization and hyphal length. This outcome may be partly explained by the adequate P availability in our experiment. Arbuscular mycorrhizal symbiosis is established by the allocation of photosynthetic C from the plant to the fungus, and an important driver of this symbiosis is low bioavailability of soil P (Leake and Read, 2017). In the present study, P availability was likely enhanced by fertilizer addition, reducing the plant's dependence on AMF-mediated nutrient acquisition. Consequently, plants may have allocated less C to the symbiosis, limiting fungal development and potentially explaining why basalt amendment did not increase AMF colonization or hyphal length.

In addition, the short experimental duration of our trial (113 days) might have constrained the potential for AMF to influence crop yield and quality. Indeed, a meta-analysis by Qin et al. (2022) identified experimental duration as the most important factor limiting the influence of AMF on crop growth, followed by soil texture, with a smaller AMF effect on sandy soils (>50 % sand). Given both the short experimental duration of the present experiment and texture of the used soil (sandy loam; 69.5 % sand), it is likely that both factors played a role in the observed lack of AMF effect on plant biomass in our study. Although a longer experimental duration might have allowed both basalt- and AMF-mediated responses to develop more fully, extending the study was not feasible because the pasteurized, AMF-free mesocosms would eventually have been recolonized by AMF spores, thereby compromising the integrity of the AMF-free treatment.

Finally, soil pasteurization likely removed a substantial fraction of the indigenous microbial community, potentially limiting the extent to which basalt-induced improvements in soil chemistry could translate into plant responses. Many beneficial effects of increased soil pH on plant growth and nutrition are mediated by soil microorganisms through processes such as organic matter decomposition and consequent nutrient mineralization, solubilization, and uptake (Richardson et al., 2009; Van Der Heijden et al., 2008). Moreover, soil pH is a major determinant of microbial community composition and activity (Fierer and Jackson, 2006; Lauber et al., 2009), meaning that microbial responses to pH change represent an important pathway through which basalt can influence nutrient cycling and crop performance. By substantially reducing microbial

585 abundance and diversity, pasteurization may therefore have disrupted these microbial pathways, weakening the link between basalt-induced increases in pH and improvements in nutrient availability. Consequently, the reduced microbial community may have contributed to the limited crop responses observed, despite clear changes in soil chemical properties.

The observed lack of a plant biomass response is similar to results by Vienne et al. (2022), where the application of 50 ton
590 ha^{-1} of basalt did not significantly affect potato growth. In other experiments, on the other hand, basalt application increased biomass of spring oat (Skov et al., 2024), sorghum (Kelland et al., 2020), and maize (Rijnders et al., 2025). Additional counter evidence is provided by the review of Swoboda et al. (2022), which focused primarily on silicate rock powder applications in highly weathered, nutrient-poor soils, and which reported a positive silicate effect on crop biomass for almost all studies using mafic and ultramafic rocks as feedstock. Taken together with previous studies, our results indicate that
595 positive crop responses to basalt are not universal and may be small or absent in relatively fertile soils such as the one studied here. The contrasting responses reported across soils and regions emphasize the context dependency of EW outcomes. In our experiment, plant N:P ratios (around 7.7; Fig. S7) suggest that crop growth remained primarily constrained by N rather than P availability. Because basalt amendments supply base cations and, to a lesser extent, P, but do not contribute to biologically available N, their potential to alleviate the dominant nutrient limitation in our system was
600 inherently limited. In contrast, EW may deliver greater agronomic benefits in highly weathered tropical soils, where soil acidity, low base saturation, and depletion of rock-derived nutrients are more common and where basalt-derived nutrient inputs can more directly alleviate nutrient constraints (Haque et al., 2025; Swoboda et al., 2022).

4.4 Need for monitoring of toxic trace elements

Our findings highlight the need for careful monitoring of soil and plant heavy metal concentrations following basalt
605 amendment. Given the observed increases in pore water Zn and Ni, our results do not support the hypothesis that basalt application does not elevate the availability of heavy metals in the soil. This is noteworthy, as Ni release is among the primary environmental safety concerns associated with EW in agricultural contexts (Suhrhoff, 2022; Te Pas et al., 2023). During the 113-day experimental period, average pore water Ni concentrations exceeded the freshwater Environmental Quality Standards (EQS) of both the European Union (EU; 4 $\mu g\ l^{-1}$) and Australia (0.3-10 $\mu g\ l^{-1}$, depending on water pH and
610 hardness) in both the control and basalt treatments (7.1 ± 1.7 and 19.7 ± 4.9 $\mu g\ l^{-1}$, respectively) (Anzg, 2024; European Commission, 2006). This may be partly due to background soil Ni levels. Nevertheless, the observed concentrations remained below the regulatory limits set by other jurisdictions, such as the United States (52 and 470 $\mu g\ l^{-1}$ for chronic and acute exposure, respectively) and Canada (3-150 $\mu g\ l^{-1}$, depending on water hardness) (B.C. Ministry of Water, 2024; Canadian Council of Ministers of the Environment, 1987; Epa, 1995).

615

Plant heavy metal concentrations were generally unaffected by basalt amendment, with the notable exception of an increase in Ni in corn tissue (0.42 ± 0.0001 and 0.65 ± 0.0004 mg kg^{-1} for control –AMF and basalt +AMF respectively), therefore

only partially supporting the hypothesis that basalt amendment does not increase plant heavy metal concentrations. Despite the increase, corn Ni concentrations remained below the EU regulatory threshold of 0.8 mg kg^{-1} which will come into effect in 2026 (European Commission, 2024). Our results therefore partially contrast with previous research, where Ni concentrations did not increase upon basalt application (Kelland et al., 2020; Rijnders et al., 2025; Vienne et al., 2022).

Heavy metal concentrations in the pore water and soil exchangeable complex were mostly not affected by AMF. On the other hand, AMF increased Cr concentration in the corn tissue. Therefore, our hypothesis that AMF presence would modulate heavy metal availability is only partially supported by our data. It is important to note that Cr concentrations in corn tissue were, regardless of treatment, higher than the average Cr concentrations found in common vegetables as identified by WHO (World Health Organization, 1988), which is in the range of 0.005-0.03 mg Cr kg^{-1} fresh weight (Fig. S14). This finding suggests that AMF inoculation does not universally confer benefits and may, under certain conditions, such as in co-deployment with silicate amendment in soils with elevated background Cr contents, pose risks to food safety.

5 Conclusion

Despite an interaction effect of basalt and arbuscular mycorrhizal fungi (AMF) on pore water dissolved inorganic carbon (DIC), our 113-day mesocosm experiment did not reveal a significant AMF-induced enhancement of weathering rates, as assessed through cation mass balance, pore water alkalinity and pore water pH. These findings suggest that pore water DIC alone is not a reliable proxy for weathering dynamics in soil systems, given its sensitivity to a range of dynamic soil parameters such as partial CO_2 pressure and pH. Notably, under the relatively nutrient-rich conditions of this study, AMF had limited influence on nutrient availability, crop yield and quality. Longer-term experiments or those conducted under nutrient-limited conditions are needed to verify whether this lack of a short-term effect persists over time.

In contrast to AMF, basalt amendment improved several indicators of chemical soil fertility, including soil pH, cation exchange capacity (CEC) and base saturation (particularly exchangeable Ca and Mg). These findings support the role of enhanced weathering in mitigating soil acidification and restoring base cation availability. However, these improvements did not translate into enhanced crop yield or nutrient status, with the exception of increased Mg concentrations in plant tissues. Our results therefore suggest limited short-term agronomic benefits of basalt amendment in this experiment, which used a fertilized sandy loam soil with relatively high nutrient availability and only moderate acidity. Moreover, although the increase of toxic trace elements in soil and plants was limited, our results stress the importance of carefully evaluating the environmental safety of enhanced weathering for the soil under consideration.

Code and data availability

The data and model code in support of our findings are openly available in Zenodo at https://doi.org/10.5281/zenodo.16813184 (Boito, 2025).

Author contributions

LB and JR contributed equally to this manuscript. LB and JR: conceptualization, data curation, formal analysis, investigation, project administration, software, supervision, visualization, writing – original draft, writing – review and editing. LS: conceptualization, data curation, formal analysis, funding acquisition, investigation, software, methodology, project administration, supervision, writing – review and editing. PF: investigation, methodology, writing – review and editing. MM: investigation, writing – review and editing. AV: conceptualization, formal analysis, funding acquisition, software, writing – review and editing. EV: methodology, writing – review and editing. SV: conceptualization, formal analysis, funding acquisition, methodology, project administration, resources, supervision, writing – review and editing.

Competing interests

The authors declare that they have no conflict of interest.

Acknowledgements

We thank Emma Pellegrini, Martín "Gato" Carrera Larrea, Sarah Janse and Jasper Roussard for their invaluable contributions during data collection. We thank the Helmholtz Laboratory for the Geochemistry of the Earth Surface (HELGES) for carrying out elemental analyses of the pore water and the sequential extraction protocol of soil samples.

Financial support

This project has received funding from Fonds Research Foundation-Flanders (FWO), project Grants No G000821N, G0A4821N; and from the University of Antwerp, Grant No FN 5423001. A.V. and L.S. were financially supported by the Fonds Research Foundation Flanders (FWO) Ph.D. Fellowship (Grant Nos 1S06325N and 1174925N respectively).

References

Akortey, W., Oppong Danso, E., Dietzen, C., Amponsah, W., Arthur, E., Boadi Mensah, B. K., Obour, P. B., Nyasapoh, J. B. A., Darko, D. A., Dorvlo, S. Y., Sabi, E. B., Abenney-Mickson, S., and Rosing, M. T.: Short-term effects of Greenlandic glacial rock flour on soil physical properties and maize yield, Nutrient Cycling in Agroecosystems, 132, 10.1007/s10705-025-10452-2, 2026.

Amann, T., Hartmann, J., Struyf, E., de Oliveira Garcia, W., Fischer, E. K., Janssens, I., Meire, P., and Schoelynck, J.: Enhanced Weathering and related element fluxes – a cropland mesocosm approach, Biogeosciences, 17, 103-119, 10.5194/bg-17-103-2020, 2020.

Anda, M., Shamshuddin, J., and Fauziah, C. I.: Improving chemical properties of a highly weathered soil using finely ground basalt rocks, Catena, 124, 147-161, 10.1016/j.catena.2014.09.012, 2015.

ANZG: Toxicant default guideline values for aquatic ecosystem protection: Nickel in freshwater., 2024.

B.C. Ministry of Water, L., and Resources Stewardship;: Nickel Water Quality Guideline for the Protection of Freshwater Aquatic Life-Technical Report, 2024.

Basile-Doelsch, I., Balesdent, J., and Rose, J.: Are interactions between organic compounds and nanoscale weathering minerals the key drivers of carbon storage in soils?, Environ Sci Technol, 49, 3997-3998, 10.1021/acs.est.5b00650, 2015.

Basta, N., Pantone, D., and Tabatabai, M.: Path analysis of heavy metal adsorption by soil, Agronomy Journal, 85, 1054-1057, https://doi.org/10.2134/agronj1993.00021962008500050018x, 1993.

Beerling, D. J., Kantzas, E. P., Lomas, M. R., Wade, P., Eufrasio, R. M., Renforth, P., Sarkar, B., Andrews, M. G., James, R. H., Pearce, C. R., Mercure, J. F., Pollitt, H., Holden, P. B., Edwards, N. R., Khanna, M., Koh, L., Quegan, S., Pidgeon, N. F., Janssens, I. A., Hansen, J., and Banwart, S. A.: Potential for large-scale CO(2) removal via enhanced rock weathering with croplands, Nature, 583, 242-248, 10.1038/s41586-020-2448-9, 2020.

Bijma, J., Hagens, M., Hammes, J., Planavsky, N., Pogge von Strandmann, P. A. E., Reershemius, T., Reinhard, C. T., Renforth, P., Suhrhoff, T. J., Vicca, S., Vienne, A., and Wolf-Gladrow, D. A.: Reviews and syntheses: Carbon vs. cation based MRV of Enhanced Rock Weathering and the issue of soil organic carbon, EGUsphere, 10.5194/egusphere-2025-2740, 2025.

Blume, H. P., Brümmer, G. W., Horn, R., Kandeler, E., Kögel-Knabner, I., Kretzschmar, R., Stahr, K., Wilke, B.-M., Thiele-Bruhn, S., and Welp, G.: Scheffer/schachtschabel, Lehrbuch der Bodenkunde, 16, 10-1007, 2010.

Boito, L. R., J.; Steinwidder, L.; Frings, P.; Maes, M.; Vienne, A.; Verbruggen, E.; Vicca, S.: Effects of basalt amendment and mycorrhizal inoculation on soil chemical properties and maize growth (1), Zenodo [dataset], https://doi.org/10.5281/zenodo.16813184, 2025.

Boniao, R. D., Shamshuddin, J., Van Ranst, E., Zauyah, S., and Syed Omar, S. R.: Changes in chemical properties and growth of corn in volcanic soils treated with peat, ground basalt pyroclastics, and calcium silicate, Communications in Soil Science and Plant Analysis, 33, 1219-1233, 10.1081/css-120003883, 2006.

Brown, I. C.: A rapid method of determining exchangeable hydrogen and total exchangeable bases of soils, Soil Science, 56, 353-358, 1943.

Buss, W., Hasemer, H., Ferguson, S., and Borevitz, J.: Stabilisation of soil organic matter with rock dust partially counteracted by plants, Glob Chang Biol, 30, e17052, 10.1111/gcb.17052, 2023.

Buss, W., Hasemer, H., Sokol, N. W., Rohling, E. J., and Borevitz, J.: Applying minerals to soil to draw down atmospheric carbon dioxide through synergistic organic and inorganic pathways, Communications Earth & Environment, 5, 10.1038/s43247-024-01771-3, 2024.

Water Quality Guidelines for the Protection of Aquatic Life: https://ccme.ca/en/chemical/139, last access: 06/03/2026.

Clough, G. H., Blatchford, S., and Hamm, P. B.: Common smut reduces sweet corn yield and ear processing quality, HortScience, 46, 1507-1511, 10.21273/HORTSCI.46.11.1507, 2011.

Conceição, L. T., Silva, G. N., Holsback, H. M. S., Oliveira, C. d. F., Marcante, N. C., Martins, É. d. S., Santos, F. L. d. S., and Santos, E. F.: Potential of basalt dust to improve soil fertility and crop nutrition, Journal of Agriculture and Food Research, 10, 10.1016/j.jafr.2022.100443, 2022.

DeMaster, D. J.: The supply and accumulation of silica in the marine environment, Geochimica et Cosmochimica acta, 45, 1715-1732, https://doi.org/10.1016/0016-7037(81)90006-5, 1981.

Departement Landbouw & Visserij: Bemestingstechnieken Organische Mest, MACHINEDEMONSTRATIE BEMESTINGSTECHNIEKEN ORGANISCHE MEST, Merelbeke, Belgium,
Desmalles, C., Jordan-Meille, L., Hernandez, J., Thomas, C. L., Dunham, S., Deng, F., McGrath, S. P., and Haefele, S. M.: Impact of Basalt Rock Powder on Ryegrass Growth and Nutrition on Sandy and Loamy Acid Soils, Agronomy, 15, 10.3390/agronomy15081791, 2025.
Dietzen, C., Harrison, R., and Michelsen-Correa, S.: Effectiveness of enhanced mineral weathering as a carbon sequestration tool and alternative to agricultural lime: An incubation experiment, International Journal of Greenhouse Gas Control, 74, 251-258, 10.1016/j.ijggc.2018.05.007, 2018.
Dinno, A.: _dunn.test: Dunn'sTest of Multiple Comparisons Using Rank Sums_ (R package version 1.3.6) [code], 2024.
Dupla, X., Möller, B., Baveye, P. C., and Grand, S.: Potential accumulation of toxic trace elements in soils during enhanced rock weathering, European Journal of Soil Science, 74, 10.1111/ejss.13343, 2023.
Dupla, X., Brantley, S.L., Paulo, C., Möller, B., Power, I.M., Grand, S.: Geochemical Drivers of Enhanced Rock Weathering in Soils, in: Geoengineering and Climate Change, edited by: Beech, M., https://doi.org/10.1002/9781394204847.ch13, 2025.
National Recommended Water Quality Criteria - Aquatic Life Criteria Table: https://www.epa.gov/wqc/national-recommended-water-quality-criteria-aquatic-life-criteria-table#table, last access: 06/03/2026.
European Commission: COMMISSION REGULATION (EC) No 1881/2006 of 19 December 2006 setting maximum levels for certain contaminants in foodstuffs, 2006.
European Commission: COMMISSION REGULATION (EU) 2024/1987 of 30 July 2024 amending Regulation (EU) 2023/915 as regards maximum levels of nickel in certain foodstuffs, 2024.
Ferrol, N., Azcon-Aguilar, C., and Perez-Tienda, J.: Review: Arbuscular mycorrhizas as key players in sustainable plant phosphorus acquisition: An overview on the mechanisms involved, Plant Sci, 280, 441-447, 10.1016/j.plantsci.2018.11.011, 2019.
Fierer, N. and Jackson, R. B.: The diversity and biogeography of soil bacterial communities, Proceedings of the National Academy of Sciences, 103, 626-631, https://doi.org/10.1073/pnas.0507535103, 2006.
Gillman, G.: The effect of crushed basalt scoria on the cation exchange properties of a highly weathered soil, Soil Science Society of America Journal, 44, 465-468, https://doi.org/10.2136/sssaj1980.03615995004400030005x, 1980.
Gillman, G., Burkett, D., and Coventry, R.: A laboratory study of application of basalt dust to highly weathered soils: effect on soil cation chemistry, Soil Research, 39, 799-811, https://doi.org/10.1071/SR00073, 2001.
Gillman, G., Burkett, D., and Coventry, R.: Amending highly weathered soils with finely ground basalt rock, Applied Geochemistry, 17, 987-1001, https://doi.org/10.1016/S0883-2927(02)00078-1, 2002.
Giovannetti, M. and Mosse, B.: An Evaluation of Techniques for Measuring Vesicular Arbuscular Mycorrhizal Infection in Roots, New Phytologist, 84, 489-500, 10.1111/j.1469-8137.1980.tb04556.x, 2006.
Goll, D. S., Ciais, P., Amann, T., Buermann, W., Chang, J., Eker, S., Hartmann, J., Janssens, I., Li, W., Obersteiner, M., Penuelas, J., Tanaka, K., and Vicca, S.: Potential CO2 removal from enhanced weathering by ecosystem responses to powdered rock, Nature Geoscience, 14, 545-549, 10.1038/s41561-021-00798-x, 2021.
Gonzalez-Chavez, M. C., Carrillo-Gonzalez, R., Wright, S. F., and Nichols, K. A.: The role of glomalin, a protein produced by arbuscular mycorrhizal fungi, in sequestering potentially toxic elements, Environ Pollut, 130, 317-323, 10.1016/j.envpol.2004.01.004, 2004.
Goudie, A. S. and Viles, H. A.: Weathering and the global carbon cycle: Geomorphological perspectives, Earth-Science Reviews, 113, 59-71, 10.1016/j.earscirev.2012.03.005, 2012.
Gudbrandsson, S., Wolff-Boenisch, D., Gislason, S. R., and Oelkers, E. H.: An experimental study of crystalline basalt dissolution from 2 $\leqslant$ pH $\leqslant$ 11 and temperatures from 5 to 75 °C, Geochimica et Cosmochimica Acta, 75, 5496-5509, 10.1016/j.gca.2011.06.035, 2011.
Guo, W., Nazim, H., Liang, Z., and Yang, D.: Magnesium deficiency in plants: An urgent problem, The Crop Journal, 4, 83-91, 10.1016/j.cj.2015.11.003, 2016.
Haque, F., Möller, B., Sagina, S., Odhiambo, C., Ondolo, H., Thuo, N., Kamau, K., and Davies, S.: Agronomic Performance of Enhanced Rock Weathering in a Tropical Smallholder System: A Maize Trial in Kenya, CDRXIV, https://doi.org/10.70212/cdrxiv.2025410.v1, 2025.

Hartmann, J., West, A. J., Renforth, P., Köhler, P., De La Rocha, C. L., Wolf-Gladrow, D. A., Dürr, H. H., and Scheffran, J.: Enhanced chemical weathering as a geoengineering strategy to reduce atmospheric carbon dioxide, supply nutrients, and mitigate ocean acidification, Reviews of Geophysics, 51, 113-149, 10.1002/rog.20004, 2013.

Iff, N., Renforth, P., and Pogge von Strandmann, P. A. E.: The dissolution of olivine added to soil at 32°C: the fate of weathering products and its implications for enhanced weathering at different temperatures, Frontiers in Climate, 6, 10.3389/fclim.2024.1252210, 2024.

Johnson, N. C., Rowland, D. L., Corkidi, L., Egerton-Warburton, L. M., and Allen, E. B.: Nitrogen enrichment alters mycorrhizal allocation at five mesic to semiarid grasslands, Ecology, 84, 1895-1908, https://doi.org/10.1890/0012-9658(2003)084[1895:NEAMAA]2.0.CO;2, 2003.

Kalamulla, R., Karunarathna, S. C., Tibpromma, S., Galappaththi, M. C. A., Suwannarach, N., Stephenson, S. L., Asad, S., Salem, Z. S., and Yapa, N.: Arbuscular Mycorrhizal Fungi in Sustainable Agriculture, Sustainability, 14, 10.3390/su141912250, 2022.

Kelland, M. E., Wade, P. W., Lewis, A. L., Taylor, L. L., Sarkar, B., Andrews, M. G., Lomas, M. R., Cotton, T. E. A., Kemp, S. J., James, R. H., Pearce, C. R., Hartley, S. E., Hodson, M. E., Leake, J. R., Banwart, S. A., and Beerling, D. J.: Increased yield and CO(2) sequestration potential with the C(4) cereal Sorghum bicolor cultivated in basaltic rock dust-amended agricultural soil, Glob Chang Biol, 26, 3658-3676, 10.1111/gcb.15089, 2020.

Kleber, M., Eusterhues, K., Keiluweit, M., Mikutta, C., Mikutta, R., and Nico, P. S.: Mineral–Organic Associations: Formation, Properties, and Relevance in Soil Environments, in, Advances in Agronomy, 1-140, 10.1016/bs.agron.2014.10.005, 2015.

Koele, N., Dickie, I. A., Blum, J. D., Gleason, J. D., and de Graaf, L.: Ecological significance of mineral weathering in ectomycorrhizal and arbuscular mycorrhizal ecosystems from a field-based comparison, Soil Biology and Biochemistry, 69, 63-70, 10.1016/j.soilbio.2013.10.041, 2014.

Kuznetsova, A., Brockhoff, P. B., and Christensen, R. H.: lmerTest package: tests in linear mixed effects models, Journal of statistical software, 82, 1-26, 10.18637/jss.v082.i13, 2017.

Lauber, C. L., Hamady, M., Knight, R., and Fierer, N.: Pyrosequencing-based assessment of soil pH as a predictor of soil bacterial community structure at the continental scale, Appl Environ Microbiol, 75, 5111-5120, 10.1128/AEM.00335-09, 2009.

Leake, J. R. and Read, D. J.: Mycorrhizal Symbioses and Pedogenesis Throughout Earth's History, in: Mycorrhizal Mediation of Soil, 9-33, 10.1016/b978-0-12-804312-7.00002-4, 2017.

Lei, K., Bucka, F. B., Teixeira, P. P. C., Buegger, F., Just, C., and Kogel-Knabner, I.: Balancing Organic and Inorganic Carbon Dynamics in Enhanced Rock Weathering: Implications for Carbon Sequestration, Glob Chang Biol, 31, e70186, 10.1111/gcb.70186, 2025.

Lewis, A. L., Sarkar, B., Wade, P., Kemp, S. J., Hodson, M. E., Taylor, L. L., Yeong, K. L., Davies, K., Nelson, P. N., Bird, M. I., Kantola, I. B., Masters, M. D., DeLucia, E., Leake, J. R., Banwart, S. A., and Beerling, D. J.: Effects of mineralogy, chemistry and physical properties of basalts on carbon capture potential and plant-nutrient element release via enhanced weathering, Applied Geochemistry, 132, 10.1016/j.apgeochem.2021.105023, 2021.

Li, J.-G. and Dong, Y.-H.: Effect of a rock dust amendment on disease severity of tomato bacterial wilt, Antonie Van Leeuwenhoek, 103, 11-22, https://doi.org/10.1007/s10482-012-9781-4, 2013.

Maathuis, F. J. and Amtmann, A.: K+ nutrition and Na+ toxicity: the basis of cellular K+/Na+ ratios, Annals of botany, 84, 123-133, https://doi.org/10.1006/anbo.1999.0912, 1999.

Malmström, M. E., Destouni, G., Banwart, S. A., and Strömberg, B. H.: Resolving the scale-dependence of mineral weathering rates, Environmental science & technology, 34, 1375-1378, https://doi.org/10.1021/es990682u, 2000.

Manning, D. A. C., de Azevedo, A. C., Zani, C. F., and Barneze, A. S.: Soil carbon management and enhanced rock weathering: The separate fates of organic and inorganic carbon, European Journal of Soil Science, 75, 10.1111/ejss.13534, 2024.

Matei, A. and Doehlemann, G.: Cell biology of corn smut disease-Ustilago maydis as a model for biotrophic interactions, Curr Opin Microbiol, 34, 60-66, 10.1016/j.mib.2016.07.020, 2016.

Miller, R., Jastrow, J., and Reinhardt, D.: External hyphal production of vesicular-arbuscular mycorrhizal fungi in pasture and tallgrass prairie communities, Oecologia, 103, 17-23, https://doi.org/10.1007/BF00328420, 1995.

Moosdorf, N., Renforth, P., and Hartmann, J.: Carbon dioxide efficiency of terrestrial enhanced weathering, Environ Sci Technol, 48, 4809-4816, 10.1021/es4052022, 2014.
Moretti, L. G., Bossolani, J. W., Crusciol, C. A. C., Moreira, A., Micheri, P. H., Rossi, R., and Imaizumi, C.: Dunite in Agriculture: Physiological Changes, Nutritional Status and Soybean Yield, Communications in Soil Science and Plant Analysis, 50, 1775-1784, 10.1080/00103624.2019.1635143, 2019.
Moyano, F., Kutsch, W., and Schulze, E.: Response of mycorrhizal, rhizosphere and soil basal respiration to temperature and photosynthesis in a barley field, Soil Biology and Biochemistry, 39, 843-853, 10.1016/j.soilbio.2006.10.001, 2007.
Neumann, E. and George, E.: Nutrient Uptake: The Arbuscular Mycorrhiza Fungal Symbiosis as a Plant Nutrient Acquisition Strategy, in: Arbuscular Mycorrhizas: Physiology and Function, 137-167, 10.1007/978-90-481-9489-6_7, 2010.
Niron, H., Vienne, A., Frings, P., Poetra, R., and Vicca, S.: Exploring the synergy of enhanced weathering and Bacillus subtilis: A promising strategy for sustainable agriculture, Glob Chang Biol, 30, e17511, 10.1111/gcb.17511, 2024.
Oldfield, E. E., Bradford, M. A., and Wood, S. A.: Global meta-analysis of the relationship between soil organic matter and crop yields, Soil, 5, 15-32, 10.5194/soil-5-15-2019, 2019.
Palandri, J. L. and Kharaka, Y. K.: A compilation of rate parameters of water-mineral interaction kinetics for application to geochemical modeling, US Geological Survey2331-1258, https://doi.org/10.3133/ofr20041068, 2004.
Parniske, M.: Arbuscular mycorrhiza: the mother of plant root endosymbioses, Nat Rev Microbiol, 6, 763-775, 10.1038/nrmicro1987, 2008.
Perez-Fodich, A. and Derry, L. A.: Organic acids and high soil CO2 drive intense chemical weathering of Hawaiian basalts: Insights from reactive transport models, Geochimica et Cosmochimica Acta, 249, 173-198, 10.1016/j.gca.2019.01.027, 2019.
Pinheiro, J., Bates, D., DebRoy, S., Sarkar, D., and Team, R. C.: Linear and nonlinear mixed effects models, R package version, 3, 1-89, 2007.
Qin, M., Li, L., Miranda, J. P., Tang, Y., Song, B., Oosthuizen, M. K., and Wei, W.: Experimental duration determines the effect of arbuscular mycorrhizal fungi on plant biomass in pot experiments: A meta-analysis, Front Plant Sci, 13, 1024874, 10.3389/fpls.2022.1024874, 2022.
Quirk, J., Leake, J. R., Johnson, D. A., Taylor, L. L., Saccone, L., and Beerling, D. J.: Constraining the role of early land plants in Palaeozoic weathering and global cooling, Proc Biol Sci, 282, 20151115, 10.1098/rspb.2015.1115, 2015.
R Core Team: RStudio: Integrated Development Environment for R (2024.4.2.764), Posit Software PBC [code], 2024.
Renforth, P., Washbourne, C. L., Taylder, J., and Manning, D. A.: Silicate production and availability for mineral carbonation, Environ Sci Technol, 45, 2035-2041, 10.1021/es103241w, 2011.
Riaz, M., Kamran, M., Fang, Y., Wang, Q., Cao, H., Yang, G., Deng, L., Wang, Y., Zhou, Y., Anastopoulos, I., and Wang, X.: Arbuscular mycorrhizal fungi-induced mitigation of heavy metal phytotoxicity in metal contaminated soils: A critical review, J Hazard Mater, 402, 123919, 10.1016/j.jhazmat.2020.123919, 2021.
Richardson, A. E., Barea, J.-M., McNeill, A. M., and Prigent-Combaret, C.: Acquisition of phosphorus and nitrogen in the rhizosphere and plant growth promotion by microorganisms, Plant and Soil, 321, 305-339, 10.1007/s11104-009-9895-2, 2009.
Righi, D. and Meunier, A.: Origin of Clays by Rock Weathering and Soil Formation, in: Origin and Mineralogy of Clays, Springer-Verlag, Berlin, https://doi.org/10.1007/978-3-662-12648-6_3, 1995.
Rijnders, J., Vienne, A., and Vicca, S.: Effects of basalt, concrete fines, and steel slag on maize growth and toxic trace element accumulation in an enhanced weathering experiment, Biogeosciences, 22, 2803-2829, 10.5194/bg-22-2803-2025, 2025.
Rijnders, J., Vicca, S., Struyf, E., Amann, T., Hartmann, J., Meire, P., Janssens, I., and Schoelynck, J.: The effects of dunite fertilization on growth and elemental composition of barley and wheat differ with dunite grain size and rainfall regimes, Frontiers in Environmental Science, 11, 10.3389/fenvs.2023.1172621, 2023.
Rillig, M. C., Field, C. B., and Allen, M. F.: Soil biota responses to long-term atmospheric CO2 enrichment in two California annual grasslands, Oecologia, 119, 572-577, https://doi.org/10.1007/s004420050821, 1999.
Rillig, M. C., Aguilar-Trigueros, C. A., Bergmann, J., Verbruggen, E., Veresoglou, S. D., and Lehmann, A.: Plant root and mycorrhizal fungal traits for understanding soil aggregation, New Phytologist, 205, 1385-1388, https://www.jstor.org/stable/newphytologist.205.4.1385, 2015.

Roy, R. and Finck, A.: Plant nutrition for food security-A guide for integrated nutrient management, FAO Knowledge Repository2006.
Klimatologische overzichten van 2022: https://www.meteo.be/nl/klimaat/klimaat-van-belgie/klimatologisch-overzicht/2022/zomer, last
Rusco, E., Jones, R. J., and Bidoglio, G.: Organic matter in the soils of Europe: Present status and future trends, Institute for Environment and Sustainability, Joint Research Centre …2001.
Saccone, L., Conley, D., Koning, E., Sauer, D., Sommer, M., Kaczorek, D., Blecker, S., and Kelly, E.: Assessing the extraction and quantification of amorphous silica in soils of forest and grassland ecosystems, European Journal of Soil Science, 58, 1446-1459, https://doi.org/10.1111/j.1365-2389.2007.00949.x, 2007.
Shamshuddin, J., Anda, M., Fauziah, C., and Omar, S. S.: Growth of cocoa planted on highly weathered soil as affected by application of basalt and/or compost, Communications in soil science and plant analysis, 42, 2751-2766, https://doi.org/10.1080/00103624.2011.622822, 2011.
Skov, K., Wardman, J., Healey, M., McBride, A., Bierowiec, T., Cooper, J., Edeh, I., George, D., Kelland, M. E., Mann, J., Manning, D., Murphy, M. J., Pape, R., Teh, Y. A., Turner, W., Wade, P., and Liu, X.: Initial agronomic benefits of enhanced weathering using basalt: A study of spring oat in a temperate climate, PLoS One, 19, e0295031, 10.1371/journal.pone.0295031, 2024.
Slessarev, E. W., Chadwick, O. A., Sokol, N. W., Nuccio, E. E., and Pett-Ridge, J.: Rock weathering controls the potential for soil carbon storage at a continental scale, Biogeochemistry, 157, 1-13, 10.1007/s10533-021-00859-8, 2021.
Smith, S. E. and Read, D. J.: Mycorrhizal symbiosis, Academic press2010.
Smith, S. E., Jakobsen, I., Grønlund, M., and Smith, F. A.: Roles of arbuscular mycorrhizas in plant phosphorus nutrition: interactions between pathways of phosphorus uptake in arbuscular mycorrhizal roots have important implications for understanding and manipulating plant phosphorus acquisition, Plant physiology, 156, 1050-1057, https://doi.org/10.1104/pp.111.174581, 2011.
Smits, M. M. and Wallander, H.: Role of Mycorrhizal Symbiosis in Mineral Weathering and Nutrient Mining from Soil Parent Material, in: Mycorrhizal Mediation of Soil, 35-46, 10.1016/b978-0-12-804312-7.00003-6, 2017.
Sochorová, L., Jansa, J., Verbruggen, E., Hejcman, M., Schellberg, J., Kiers, E. T., and Johnson, N. C.: Long-term agricultural management maximizing hay production can significantly reduce belowground C storage, Agriculture, Ecosystems & Environment, 220, 104-114, 10.1016/j.agee.2015.12.026, 2016.
Steinwidder, L., Boito, L., Frings, P. J., Niron, H., Rijnders, J., de Schutter, A., Vienne, A., and Vicca, S.: Beyond Inorganic C: Soil Organic C as a Key Pathway for Carbon Sequestration in Enhanced Weathering, Glob Chang Biol, 31, e70340, 10.1111/gcb.70340, 2025.
Strawn, D. G., Bohn, H. L., and O'Connor, G. A.: Soil chemistry, John Wiley & Sons2019.
Suhrhoff, T. J.: Phytoprevention of Heavy Metal Contamination From Terrestrial Enhanced Weathering: Can Plants Save the Day?, Frontiers in Climate, 3, 10.3389/fclim.2021.820204, 2022.
Swoboda, P., Doring, T. F., and Hamer, M.: Remineralizing soils? The agricultural usage of silicate rock powders: A review, Sci Total Environ, 807, 150976, 10.1016/j.scitotenv.2021.150976, 2022.
Taylor, L. L., Leake, J. R., Quirk, J., Hardy, K., Banwart, S. A., and Beerling, D. J.: Biological weathering and the long-term carbon cycle: integrating mycorrhizal evolution and function into the current paradigm, Geobiology, 7, 171-191, 10.1111/j.1472-4669.2009.00194.x, 2009.
te Pas, E. E. E. M., Hagens, M., and Comans, R. N. J.: Assessment of the enhanced weathering potential of different silicate minerals to improve soil quality and sequester CO2, Frontiers in Climate, 4, 10.3389/fclim.2022.954064, 2023.
ten Berge, H. F., van der Meer, H. G., Steenhuizen, J. W., Goedhart, P. W., Knops, P., and Verhagen, J.: Olivine weathering in soil, and its effects on growth and nutrient uptake in Ryegrass (Lolium perenne L.): a pot experiment, PLoS One, 7, e42098, 10.1371/journal.pone.0042098, 2012.
Tessier, A., Campbell, P. G., and Bisson, M.: Sequential extraction procedure for the speciation of particulate trace metals, Analytical chemistry, 51, 844-851, 10.1021/ac50043a017, 1979.
Totsche, K. U., Amelung, W., Gerzabek, M. H., Guggenberger, G., Klumpp, E., Knief, C., Lehndorff, E., Mikutta, R., Peth, S., Prechtel, A., Ray, N., and Kögel-Knabner, I.: Microaggregates in soils, Journal of Plant Nutrition and Soil Science, 181, 104-136, 10.1002/jpln.201600451, 2017.

Uhlig, D. and von Blanckenburg, F.: How Slow Rock Weathering Balances Nutrient Loss During Fast Forest Floor Turnover in Montane, Temperate Forest Ecosystems, Frontiers in Earth Science, 7, 10.3389/feart.2019.00159, 2019.
UN General Assembly: Transforming our world: the 2030 Agenda for Sustainable Development, 2015.
Vaghetti Luchese, A., Pivetta, L. A., Batista, M. A., Steiner, F., Giaretta, A. d. S., and Curtis, J. C. D.: Agronomic feasibility of using basalt powder as soil nutrient remineralizer, Afr. J. Agric. Res, 17, 487-497, 10.5897/AJAR2020.15234 2021.
van der Heijden, M. G., Bardgett, R. D., and van Straalen, N. M.: The unseen majority: soil microbes as drivers of plant diversity and productivity in terrestrial ecosystems, Ecol Lett, 11, 296-310, 10.1111/j.1461-0248.2007.01139.x, 2008.
Van Straaten, P.: Farming with rocks and minerals: challenges and opportunities, Anais da Academia Brasileira de Ciências, 78, 731-747, https://doi.org/10.1590/S0001-37652006000400009 2006.
Ven, A., Verlinden, M. S., Verbruggen, E., Vicca, S., and Hart, M.: Experimental evidence that phosphorus fertilization and arbuscular mycorrhizal symbiosis can reduce the carbon cost of phosphorus uptake, Functional Ecology, 33, 2215-2225, 10.1111/1365-2435.13452, 2019.
Ven, A., Verlinden, M. S., Fransen, E., Olsson, P. A., Verbruggen, E., Wallander, H., and Vicca, S.: Phosphorus addition increased carbon partitioning to autotrophic respiration but not to biomass production in an experiment with Zea mays, Plant, Cell & Environment, 43, 2054-2065, https://doi.org/10.1111/pce.13785, 2020.
Verbruggen, E. and Toby Kiers, E.: Evolutionary ecology of mycorrhizal functional diversity in agricultural systems, Evol Appl, 3, 547-560, 10.1111/j.1752-4571.2010.00145.x, 2010.
Verbruggen, E., Struyf, E., and Vicca, S.: Can arbuscular mycorrhizal fungi speed up carbon sequestration by enhanced weathering?, Plants, People, Planet, 3, 445-453, 10.1002/ppp3.10179, 2021.
Verlinden, M. S., Ven, A., Verbruggen, E., Janssens, I. A., Wallander, H., and Vicca, S.: Favorable effect of mycorrhizae on biomass production efficiency exceeds their carbon cost in a fertilization experiment, Ecology, 99, 2525-2534, 10.1002/ecy.2502, 2018.
Vienne, A., Poblador, S., Portillo-Estrada, M., Hartmann, J., Ijiehon, S., Wade, P., and Vicca, S.: Enhanced Weathering Using Basalt Rock Powder: Carbon Sequestration, Co-benefits and Risks in a Mesocosm Study With Solanum tuberosum, Frontiers in Climate, 4, 10.3389/fclim.2022.869456, 2022.
Vienne, A., Frings, P., Poblador, S., Steinwidder, L., Rijnders, J., Schoelynck, J., Vinduskova, O., and Vicca, S.: Earthworms in an enhanced weathering mesocosm experiment: Effects on soil carbon sequestration, base cation exchange and soil CO2 efflux, Soil Biology and Biochemistry, 199, 10.1016/j.soilbio.2024.109596, 2024.
Vierheilig, H., Schweiger, P., and Brundrett, M.: An overview of methods for the detection and observation of arbuscular mycorrhizal fungi in roots†, Physiologia Plantarum, 125, 393-404, 10.1111/j.1399-3054.2005.00564.x, 2005.
Vlaamse Land Maatschappij: Normen and Richtwaarden 2026, 2026.
Wagg, C., Jansa, J., Schmid, B., and van der Heijden, M. G.: Belowground biodiversity effects of plant symbionts support aboveground productivity, Ecol Lett, 14, 1001-1009, 10.1111/j.1461-0248.2011.01666.x, 2011.
Wang, C. and Kuzyakov, Y.: Soil organic matter priming: The pH effects, Glob Chang Biol, 30, e17349, 10.1111/gcb.17349, 2024.
White, A. F. and Brantley, S. L.: The effect of time on the weathering of silicate minerals: why do weathering rates differ in the laboratory and field?, Chemical Geology, 202, 479-506, 10.1016/j.chemgeo.2003.03.001, 2003.
Wilkes, T. I.: Arbuscular Mycorrhizal Fungi in Agriculture, Encyclopedia, 1, 1132-1154, 10.3390/encyclopedia1040085, 2021.
Winnick, M. J. and Maher, K.: Relationships between CO2, thermodynamic limits on silicate weathering, and the strength of the silicate weathering feedback, Earth and Planetary Science Letters, 485, 111-120, 10.1016/j.epsl.2018.01.005, 2018.
Wolf-Gladrow, D. A., Zeebe, R. E., Klaas, C., Körtzinger, A., and Dickson, A. G.: Total alkalinity: The explicit conservative expression and its application to biogeochemical processes, Marine Chemistry, 106, 287-300, 10.1016/j.marchem.2007.01.006, 2007.
Woomer, P., Martin, A., Albrecht, A., Resck, D., and Scharpenseel, H.: The importance and management of soil organic matter in the tropics, in: The Biological Management of Tropical Soil Fertility, Wiley-Sayce, 1994.
World Health Organization: Environmental Health Criteria 61: Chromium, 1988.
Wu, S., Konhauser, K. O., Chen, B., and Huang, L.: “Reactive Mineral Sink” drives soil organic matter dynamics and stabilization, npj Materials Sustainability, 1, 10.1038/s44296-023-00003-7, 2023.

Zeebe, R. E. and Wolf-Gladrow, D. A.: Chapter 1: Equilibrium, in: CO2 IN SEAWATER: EQUILIBRIUM, KINETICS, ISOTOPES, edited by: Halpern, D., Elsevier, 2001.

Table 1: Left: basalt mineral phases obtained via XRD analysis on samples milled in ethanol for 10 minutes (Bruker D8 Advance, Cu Kα radiation at 30 mA and 40 kV, 2θ from 5° to 70°). An internal standard (10 wt% Al_2O_3) was added during sample preparation to determine amorphous phase content. Right: elemental concentrations obtained via XRF analysis, provided by RPBL.

Table 2: Treatments established in the experiment, including number of replicates and abbreviations.

Figure 1: AMF hyphal length (a), root colonization by AMF (b) and root biomass (c) of the four treatments (C-AMF = control without AMF, C+AMF = control with AMF, B-AMF = basalt without AMF, B+AMF = basalt with AMF) at the end of the experiment. Boxes represent the interquartile range (25th-75th percentile), horizontal lines indicate the median, and whiskers extend to the most extreme data points within 1.5x of the interquartile range. Points outside this range are plotted as outliers. p- and F-values from an ANOVA analysis with hyphal length, root colonization or biomass as response variables and basalt, AMF and their interaction as covariables are shown. Interactions were not significant and were excluded from the model. Statistical significance is indicated by an asterisk (*). Compliance with model assumptions of normality and homoscedasticity was ensured by square-root transformation.

Figure 2: Soil pH (a), cation exchange capacity (CEC, b) and base saturation (c) of the four treatments (C-AMF = control without AMF, C+AMF = control with AMF, B-AMF = basalt without AMF, B+AMF = basalt with AMF) at the end of the experiment. Boxes represent the interquartile range (25th-75th percentile), horizontal lines indicate the median, and whiskers extend to the most extreme data points within 1.5x of the interquartile range. Points outside this range are plotted as outliers. p- and F-values from an ANOVA analysis with pH, CEC or base saturation as response variables and basalt (B), AMF and their interaction as covariables are shown. Interactions were not significant and were excluded from the model. Statistical significance is indicated by an asterisk (*).

Figure 3: Mean pH (a), total alkalinity (b) and dissolved inorganic carbon (DIC, c) in the soil pore water during the experiment for the four treatments (C-AMF = control without AMF, C+AMF = control with AMF, B-AMF = basalt without AMF, B+AMF = basalt with AMF). Error bars represent the standard error on the mean. p- and F-values from a linear regression analysis with pH, total alkalinity or DIC as response variable and basalt (B), AMF, time (T), and their relevant interactions as covariables are shown. When interactions were not significant, they were excluded from the model and are not shown here. Interactions are indicated by carets (^), while significant relationships by an asterisk (*).

Figure 4: Pore water Al (a), Ni (b) and Zn (c) concentrations during the experiment for the four treatments (C-AMF = control without AMF, C+AMF = control with AMF, B-AMF = basalt without AMF, B+AMF = basalt with AMF). Error bars represent the standard error on the mean. p- and F-values are shown from a linear regression analysis with heavy metal concentration as response variable, and basalt (B), AMF, time (T), and their relevant interactions as covariables. When interactions were not statistically significant, they were excluded from the model and not shown here. Interactions are indicated by carets (^), while significant relationships by an asterisk (*).

Figure 5: Mean Δ soil nutrient contents (Ca, Fe, K, Mg, Na and Si) for three treatments (C+AMF = control with AMF, B-AMF = basalt without AMF, B+AMF = basalt with AMF) at the end of the growing season. Error bars represent the standard error on the mean. Nutrient contents are shown as the difference between the start and the end of the growing season, and are expressed relative to the control treatment (C-AMF = control without AMF). Soils were divided into three sampling depths (0-20 cm, 20-40 cm, 40-60 cm) for which nutrient concentrations were measured in the exchangeable fraction with the sequential extraction method after Tessier et al. (1979). p- and F-values from an ANOVA analysis with nutrient concentration as response variables, and basalt, AMF and their interaction as covariables are presented in Table S3.

Figure 6: Mean Δ soil heavy metal content (Al and Zn) for three treatments (B-AMF = basalt without AMF, B+AMF = basalt with AMF, C+AMF = control with AMF) at the end of the growing season. Error bars represent the standard error on the mean. Heavy metal contents are shown as the difference between the start and end of the growing season, and are expressed relative to the control treatment (C-AMF; control without AMF). Soils were divided into three sampling depths (0-20 cm, 20-40 cm, 40-60 cm) for which heavy metal concentration in the exchangeable fraction was measured with the sequential extraction method after Tessier et al. (1979). p- and F-values from an ANOVA analysis with nutrient concentration as response variables, and basalt, AMF and their interaction as covariables are presented in Table S3.

Figure 7: Mean basalt weathering rates for the basalt treatments calculated as the increase in base cations (Ca, Mg, K, Na) in the soil phase and in the plants between the start and the end of the experiment, and corrected for the control soil (C-AMF = control without AMF). Error bars represent the standard errors on the mean. p- and t-values from a two-sample t-test are presented.

Figure 8: Concentration of Mg (a), Ni (b) and Cr (c) in the corn, leaves, stem, tassel, and roots for the four treatments (B-AMF = basalt without AMF, B+AMF = basalt with AMF, C-AMF = control without AMF, C+AMF = control with AMF) at the end of the experiment. Boxes represent the interquartile range (25th-75th percentile), horizontal lines indicate the median, and whiskers extend to the most extreme data points within 1.5x of the interquartile range. Points outside this range are plotted as outliers. Note that for Cr and Ni, the primary axis shows the concentration in the corn, leaves, stems, and tassels while the secondary axis shows the concentration in the roots. p- and F-values are shown in Table S9. Significant

differences are indicated with a different letter, while a similar letter means no differences between those treatments. Black letters indicate basalt effects, while red letter indicate AMF effects. If no letters are shown for a combination of plant part and element, this means that there was no significant influence of basalt or AMF.